

PREPARATION OF ALGINATE CAPSULE USING TWO COAXIAL GLASS-TUBE



A Thesis Submitted in Partial Fulfillment of the Requirements  
for the Degree of Master of Science in Petrochemistry and Polymer Science  
Field of Study of Petrochemistry and Polymer Science  
Faculty of Science  
Chulalongkorn University  
Academic Year 2018  
Copyright of Chulalongkorn University

การเตรียมแคลคูลัสแอลจีเน็ตโดยใช้ท่อแก้วกลางสองชั้น



วิทยานิพนธ์นี้เป็นส่วนหนึ่งของการศึกษาตามหลักสูตรปริญญาวิทยาศาสตรมหาบัณฑิต  
สาขาวิชาปิโตรเคมีและวิทยาศาสตร์พอลิเมอร์ สาขาวิชาปิโตรเคมีและวิทยาศาสตร์พอลิเมอร์

คณะวิทยาศาสตร์ จุฬาลงกรณ์มหาวิทยาลัย

ปีการศึกษา 2561

ลิขสิทธิ์ของจุฬาลงกรณ์มหาวิทยาลัย



พานิดา วัชฌง : การเตรียมแคปซูลแอลจิเนตโดยใช้ท่อแก้วกลางสองชั้น. (

PREPARATION OF ALGINATE CAPSULE USING TWO COAXIAL GLASS-TUBE) อ.

ที่ปรึกษาหลัก : ผศ. ดร.พัฒทรา ธีรพิบูลย์เดช

เทมโป-ออกซิไดซ์แบบที่เรียเซลล์ูโลสที่ได้โดยการออกซิเดชันด้วยเทมโปเพื่อผลิตหมู่คาร์บอกซิเลตบนพื้นผิวแบบที่เรียเซลล์ูโลส TOBC มีความเป็นผลึกต่ำกว่าแต่การกระจายตัวในน้ำมากกว่าแบบที่เรียเซลล์ูโลส TOBC ถูกใช้เป็นสารเสริมแรงสำหรับการผลิตแคปซูลแอลจิเนต โดยแคปซูลแอลจิเนตที่ใช้สำหรับบรรจุน้ำมันรำข้าวสร้างจากท่อแก้วกลางสองชั้น ปัจจัยที่มีอิทธิพลต่อรูปร่างและประสิทธิภาพการผลิตของแคปซูลคือระยะห่างระหว่างปลายท่อและอ่างแคลเซียมไอออน และความหนืดของสารละลายเปลือกชั้นนอก อย่างไรก็ตามปัจจัยเหล่านี้ไม่มีผลต่อขนาดและความหนาของเปลือกของแคปซูล การเพิ่มปริมาณของ TOBC เพิ่มความชุ่มและทนต่อแรงบีบอัดของเปลือกแคปซูลและทำให้พื้นผิวของเปลือกแคปซูลเรียบ ฟิล์ม TOBC-แอลจิเนตถูกสร้างขึ้นเพื่อวิเคราะห์สมบัติของเปลือกแคปซูลได้ง่ายขึ้น ปริมาณ TOBC ที่มากขึ้นสามารถลดการหดตัวของฟิล์ม เพิ่มสมบัติเชิงกลและอัตราการซึมผ่านออกซิเจนได้ แต่ไม่มีผลต่อเสถียรภาพทางความร้อนและการซึมผ่านของไอน้ำ หมู่คาร์บอกซิเลตของ TOBC มีส่วนร่วมในการเชื่อมขวางกับแคลเซียมไอออนและทำหน้าที่โครงร่างของแอลจิเนต

จุฬาลงกรณ์มหาวิทยาลัย  
CHULALONGKORN UNIVERSITY

สาขาวิชา    ปิโตรเคมีและวิทยาศาสตร์พอลิ    ลายมือชื่อนิสิต .....

เมอร์

ปีการศึกษา   2561

ลายมือชื่อ อ.ที่ปรึกษาหลัก .....

# # 5872158523 : MAJOR PETROCHEMISTRY AND POLYMER SCIENCE

KEYWORD: Alginate capsules, Oxidized bacterial cellulose

Panida Watchanung : PREPARATION OF ALGINATE CAPSULE USING TWO COAXIAL GLASS-TUBE. Advisor: Asst. Prof. PATTARA THIRAPHIBUNDET, Ph.D.

TEMPO-Oxidized bacterial cellulose (TOBC) were obtained using TEMPO-mediated oxidation (TOBC) to produce carboxylate groups on bacterial cellulose surfaces. TOBC had lower crystallinity but better aqueous dispersion than bacterial cellulose. TOBC was used as a reinforcement agent for production alginate capsules. The alginate capsules for entrapping rice bran oil were made via a coaxial-glass tube. The factors that influenced on the shape and production efficiency of capsules were the gap between tube tip and the  $\text{Ca}^{2+}$  ions bath and the viscosity of shell solution. However, these factors had no effect on the size and shell thickness of capsules. Increasing of TOBC content enhanced the turbidity and compression strength of shell and gave smoother surface. The TOBC-alginate film was fabricated to easier characterization the shell property. More TOBC content can decrease the shrinkage of films, increase mechanical property and oxygen transmission rate, but had no effect on thermal and water vapor transmission rate. The carboxyl group of TOBC can participate crosslinking with  $\text{Ca}^{2+}$  and act as the structural construction of the alginate.

Field of Study: Petrochemistry and  
Polymer Science

Student's Signature .....

Academic Year: 2018

Advisor's Signature .....

## ACKNOWLEDGEMENTS

Firstly, I would like to express my sincere gratitude to my advisor Assistant Professor Pattara Thiraphibundet, Ph.D., for her valuable advice, supervision and assistance throughout the course of this research. I am also grateful thank to the member of thesis committee consist of Assistant Professor Warinthorn Chavasiri, Ph.D., Associate Professor Sirilux Poompradub, Ph.D. and Assistant Professor Karnthidaporn Wattanakul, Ph.D. the external examiner from Department of Mechanical Engineering Technology, College of Industrial Techonology, King Mongkut's University of Technology North Bangkok, for their valuable comments and suggestions.

I am forever thankful to PAT group, Department of Chemistry, Faculty of Science, Chulalongkorn University for their friendship and support, and for creating a cordial working environment. and I have many, many people to thank for listening to and, at times, having to tolerate me over the past three years.

Finally, my deep and sincere gratitude to my family for their continuous and unparalleled love, help and support. They selflessly encouraged me to explore new directions in life and seek my own destiny. This journey would not have been possible if not for them.



จุฬาลงกรณ์มหาวิทยาลัย  
CHULALONGKORN UNIVERSITY

Panida Watchanung

## TABLE OF CONTENTS

	Page
ABSTRACT (THAI).....	iii
ABSTRACT (ENGLISH).....	iv
ACKNOWLEDGEMENTS .....	v
TABLE OF CONTENTS .....	vi
LIST OF TABLES.....	x
LIST OF FIGURES .....	xi
CHAPTER I.....	1
Introduction .....	1
1.1 Motivation of research .....	1
CHAPTER II.....	3
THEORY AND LITERATURE REVIEWS.....	3
2.1 Alginate.....	3
2.1.1 Source and general properties.....	3
2.1.2 Alginate bead.....	4
2.1.2.1 External gelation.....	4
2.1.2.2 Internal gelation.....	6
2.1.2.3 Inverse gelation.....	6
2.2 Capsules.....	7
2.2.1 Commercial capsules.....	8
2.2.1.1 Hard capsule.....	8
2.2.1.2 Soft capsule.....	8

2.2.2 Alginate capsule .....	9
2.3 Bacterial Cellulose (BC).....	14
2.3.1 Source and general properties.....	14
2.3.2 TEMPO-oxidized cellulose .....	16
CHAPTER III .....	19
EXPERIMENTAL .....	19
3.1 Chemicals and materials .....	19
3.2 Preparation of TEMPO-oxidized bacterial cellulose (TOBC).....	19
3.3 Characterization of TEMPO-oxidized bacterial cellulose (TOBC).....	19
3.3.1 Attenuated total reflection fourier transform infrared (ATR-FTIR) spectroscopy .....	19
3.3.2 Determination degree of oxidation .....	20
3.3.3 X-ray diffraction (XRD) analysis .....	20
3.4 Preparation of rice bran oil loaded alginate capsules.....	20
3.5 Characterization of rice bran oil loaded alginate (OA) capsules .....	22
3.5.1 Surface appearance, size, and thickness.....	22
3.5.2 Mechanical property .....	22
3.6 Preparation of TOBC-alginate films.....	22
3.7 Characterization of TOBC-alginate films .....	23
3.7.1 Thickness .....	23
3.7.2 Light transmission and transparency .....	23
3.7.3 Thermal gravimetric analysis (TGA) .....	23
3.7.4 Scanning electron microscopy (SEM) analysis .....	23



3.7.5 Attenuated total reflection fourier transform infrared (ATR-FTIR) spectroscopy .....	24
3.7.6 X-ray diffraction (XRD) analysis .....	24
3.7.7 Mechanical property .....	24
3.7.8 Water vapor transmission rate (WVTR) .....	25
3.7.9 Oxygen transmission rate (OTR).....	25
3.10 Statistical Analysis.....	25
CHAPTER IV .....	26
RESULTS AND DISCUSSION.....	26
4.1 Characterization of TEMPO-oxidized bacterial cellulose (TOBC).....	26
4.1.1 FTIR analysis and determination degree of oxidation.....	26
4.1.2 X-ray diffraction (XRD) analysis .....	27
4.2 Characterization of rice bran oil loaded alginate (OA) capsules .....	27
4.2.1 Capsule formation efficiency (%CFE).....	27
4.2.2 Surface appearance, capsule size, and shell thickness .....	29
4.2.3 Mechanical property .....	31
4.3 Characterization of TOBC-alginate films .....	32
4.3.1 Thickness, transparency and mechanical property .....	32
4.3.2 Morphology and X-ray diffraction (XRD) analysis .....	33
4.3.3 FTIR analysis.....	34
4.3.4 Thermal gravimetric analysis (TGA) .....	35
4.3.5 Water vapor transmission rate (WVTR) .....	36
4.3.6 Oxygen transmission rate (OTR).....	37
CHAPTER V .....	39

CONCLUSION .....	39
REFERENCES .....	41
APPENDIX.....	47
APPENDIX A .....	48
APPENDIX B .....	49
APPENDIX C .....	50
APPENDIX D.....	51
VITA.....	53



## LIST OF TABLES

	Page
<b>Table 4.1</b> The size and thickness of capsules fabricated at different alginate shell solution and varied distances. ....	30
<b>Table 4.2</b> Thickness, transparency, tensile strength and Young's modulus of TOBC-alginate films. ....	33
<b>Table 4.3</b> The water vapor transmission (WVTR) of TOBC-alginate films.....	37
<b>Table 4.4</b> The Oxygen transmission rate (OTR) of TOBC-alginate films. ....	38



## LIST OF FIGURES

	Page
<b>Figure 2.1</b> Chemical structures of G blocks, M blocks and MG blocks in alginate [14].	3
<b>Figure 2.2</b> Binding to calcium ions by G-block in alginate and Egg-box model structure of an alginate gel formation [16].	4
<b>Figure 2.3</b> Mechanism of external gelation for bead formation: (a) alginate droplet into a Ca <sup>2+</sup> ions bath, (b) inward diffusion of calcium ions, (c) inward gelation of droplet, and (d) completed gelation [22].	5
<b>Figure 2.4</b> Mechanism of internal gelation for bead formation: (a) dispersion of alginate droplet in oil, (b) addition of acid to dissolve the calcium salt, and (c) localized gelation of droplet [22].	6
<b>Figure 2.5</b> Mechanism of inverse gelation for liquid-core capsule formation: (a) droplet containing calcium ions in contact with alginate solution, (b) outward diffusion of calcium ions, and (c) gelation at droplet interface [22].	7
<b>Figure 2.6</b> Hard capsule is created of a two piece.	8
<b>Figure 2.7</b> Manufacture soft capsules using by the rotary die method [33].	9
<b>Figure 2.8</b> Fabrication process of PLGA–alginate core–shell microspheres [8].	10
<b>Figure 2.9</b> Device of electro-coextrusion process for fabricated olive oil-loaded alginate macrocapsules (Left). photographs of the alginate macrocapsules different types of surface appearance (Right): (A) non-oily and smooth surface, (B) non-oily and rough surface, (C) oily and smooth surface, and (D) oily and rough surface [9].	11
<b>Figure 2.10</b> The schematic illustration of the microencapsulation process to obtain core–shell particle structure by co-axial prilling [10].	12
<b>Figure 2.11</b> Device of the melt coaxial electrospray (Left), and photographs of the alginate macrocapsules (Right) [11].	13

<b>Figure 2.12</b> Schematic of robust microfluidic platform for generating alginate microcapsules and Wet image of alginate microcapsules (a) and Dry image of alginate microcapsule (b) (Scale bar 200 $\mu\text{m}$ ) [36].	14
<b>Figure 2.13</b> The molecular structure of bacterial cellulose [38].	15
<b>Figure 2.14</b> TEMPO-mediated oxidation process of bacterial cellulose [50].	16
<b>Figure 2.15</b> Schematic representation of the structure of egg-box junction zones in TEMPO-mediated oxidation of cellulose/alginate/calcium system [51].	17
<b>Figure 3.1</b> Device for the fabricated alginate capsule.	21
<b>Figure 4.1</b> The process to produce carboxylate groups on BC surfaces by TEMPO-mediated oxidation.	26
<b>Figure 4.2</b> FTIR spectra of TOBC (a) and BC (b).	26
<b>Figure 4.3</b> The XRD patterns of BC and TOBC.	27
<b>Figure 4.4</b> Aqueous dispersion states of BC and TOBC.	27
<b>Figure 4.5</b> Capsule formation efficiency (%CFE) of OA capsules.	28
<b>Figure 4.6</b> Macroscopic capsules images of alginate with various TOBC contents and distance between tip tube and $\text{Ca}^{2+}$ bath.	30
<b>Figure 4.7</b> Images of fresh (a) and dry capsules (b), and dried-shell without core (c).	31
<b>Figure 4.8</b> The compression mechanical properties of the OA capsules.	31
<b>Figure 4.9</b> The transparency of TOBC-alginate films; no film (a), AT0 (b), AT0.12 (c), AT0.25 (d), AT0.50 (e), and AT0.75 (f) (film samples).	33
<b>Figure 4.10</b> Optical photos (A), SEM images (x5000) of surface morphology (B) Cross-section (x10000) (C), and XRD patterns (D) of alginate films contain 0% (a), 0.12% (b), 0.25% (c), 0.50% (d), and 0.75%w/v (e) of TOBC in 1%w/v alginate solution.	34
<b>Figure 4.11</b> FT-IR spectra of TOBC (a) and alginate films containing 0% (b), 0.12% (c), 0.25% (d), 0.50% (e), and 0.75 %w/v (f) of TOBC in 1%w/v alginate solution.	35
<b>Figure 4.12</b> DTG analysis of TOBC-alginate films.	36

## CHAPTER I

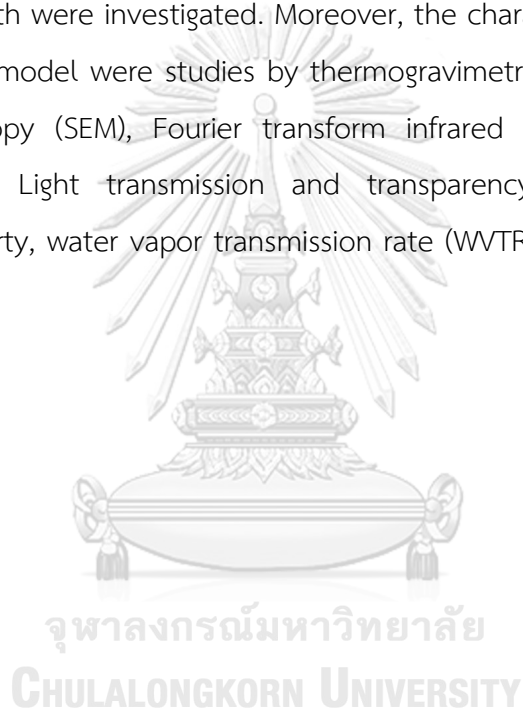
### Introduction

#### 1.1 Motivation of research

At present, gelatin is commonly used as a raw material for hard and soft capsules. Gelatin has good mechanical properties [1], thermo-reversibility, good film formability and dissolves easily at a temperature close to human body [2]. These properties make it being the appropriate material for fabricating commercial capsules. However, manufacturers use gelatin from waste pig skin due to low cost, consumers may be incurred toxic residues [3]. The alternative gelatin sources are chickens, fishes and cattle but these could not fulfill various industries demand due to high cost and halal consumers avoid bovine gelatin [4]. Moreover, consumers are concerned about the spread of diseases from animal sources of gelatin [5]. For these reasons, the alternative polymer sources from plants-derivative are interesting, such as alginate extracted from brown seaweeds. Alginate is widely used for many applications in pharmaceutical [6] and food industry [7] due to its good properties. Alginate is biocompatibility, non-toxicity, low cost, bio-degradability and gel formation ability. Alginate can form beads by ionic cross-linking with divalent cations to encapsulate a variety of substances. Its substances loading in beads are quite low because substances have to mix with excipients before forming beads. For these reasons, alginate capsules are continuously developed by techniques such as capillary microfluidic [8], electro-coextrusion [9], co-axial nozzles [10] and coaxial electrospray [11]. The fabricated capsules size is maximum 2 mm. In addition, alginate has poor mechanical property, so alginate capsules are easily broken. The incorporation of reinforcing agents into alginate is necessary to improve that property. The chemical modification of bacterial cellulose (BC) surface using 2,2,6,6-tetramethyl-1-piperidine-N-oxy radical (TEMPO) have been importance. TEMPO-oxidized cellulose is one of reinforcing agents which have reported in many studies. Moreover, the carboxyl groups on the surface of oxidized cellulose increased the

gaps between adjacent fibers as a result of the repulsive inter-action of anionic charges, which resulted in a well-solution dispersed state.

This research presents the new technique to fabricate alginate capsules. The core was loaded with rice bran oil as model. The capsules were fabricated using two coaxial glass-tube controlled with two syringe pumps. The fabricated capsules diameter was in the ranges of 4-5 mm. In addition, TEMPO-oxidized bacterial cellulose (TOBC) used as reinforcing agents to improve mechanical property of capsules shell. The capsule efficiency, surface appearance, size, and thickness and mechanical strength were investigated. Moreover, the characterization of the shell of capsules as films model were studies by thermogravimetric analysis (TGA), Scanning electron microscopy (SEM), Fourier transform infrared (FTIR) spectroscopy, X-ray diffraction (XRD), Light transmission and transparency, measurement of the mechanical property, water vapor transmission rate (WVTR) and oxygen permeability (OP).



## CHAPTER II

### THEORY AND LITERATURE REVIEWS

The purpose of this research is to fabricate rice bran oil loaded alginate capsules using two coaxial glass-tube. This process is a new method to encapsulate active compounds with simple operation. TEMPO-oxidized bacterial cellulose (TOBC) is used as reinforcing agent for improving the mechanical and thermal stability of capsule shell. This chapter presents the theory and literature reviews involved in this research.

#### 2.1 Alginate

##### 2.1.1 Source and general properties

Alginate is a hydrophilic colloidal carbohydrate extracted from various species of brown seaweeds such as *Laminaria hyperborea*, *Laminaria digitata*, *Ascophyllum nodosum*, *Macrocystis pyrifera* [12]. In molecular terms, it is composed of unbranched binary copolymers of (1-4)-linked  $\beta$ -d-mannuronic acid (M) and  $\alpha$ -l-guluronic acid (G) residues [13]. Basically, there are three types of segments namely G-block, M-block, and mixed GM-block (Fig. 2.1) [14]. Only the carboxyl functional groups of G-blocks can intermolecular cross-link with divalent cations (e.g.,  $\text{Ca}^{2+}$ ,  $\text{Sr}^{2+}$ ,  $\text{Ba}^{2+}$ ) [15], the so call egg-box model (Fig. 2.2) [16]. The M-block segments show linear and flexible configuration. For this reason, the M/G ratio affects the physicochemical properties of alginates and is used to expect the nature of gels formed from alginates [7].

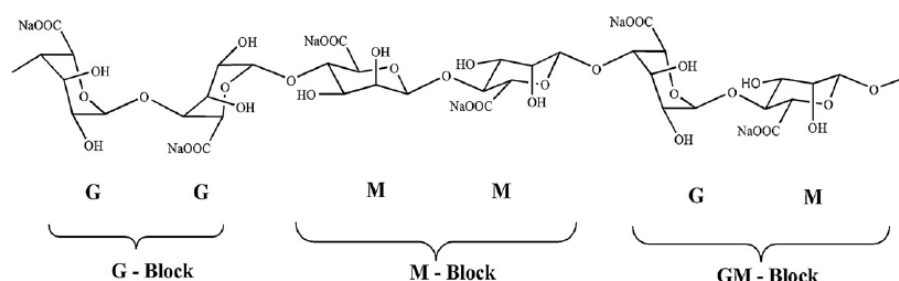


**Figure 2.1** Chemical structures of G blocks, M blocks and MG blocks in alginate [14].



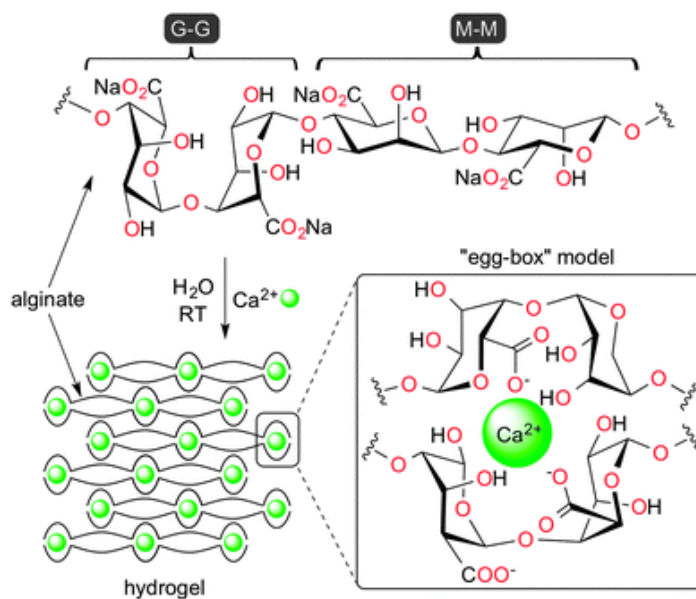


**Figure 2.2** Binding to calcium ions by G-block in alginate and Egg-box model structure of an alginate gel formation [16].

Alginates are widely used as viscosifying/gelling agents, stabilizers-thickening agent, a texture-improver and emulsifier in food industry. For examples, alginate gel formation leads to uses in jellies and instant milk desserts, fruit pies etc. [7]. Moreover, in the biomedical, cosmetic, and pharmaceutical industries, alginate hydrogels are used as wound healing, tissue engineering, matrix for drug encapsulation [6], and cells/delivery vehicle of drugs [17, 18].

### 2.1.2 Alginate bead

Alginate bead is used to encapsulate or entrap a variety of cargos, such as cells, enzymes, and active compounds. Alginate beads can be produced by many techniques, such as external, internal, and inverse gelation. This review provides an overview of this gelatinization.

#### 2.1.2.1 External gelation

External gelation is the most widely used method for fabricating alginate bead. In this method, alginate solution containing active compounds (cargo) is extruded and dropped into divalent ion solution e.g. CaCl<sub>2</sub> (Fig. 2.3). Ca<sup>2+</sup> ions diffuse into alginate droplets to initiate cross-linking bead surface leading to less penetrates

to the diffusion of  $\text{Ca}^{2+}$  into the interior. Consequently, alginate beads demonstrate a relatively less cross-linked interior and a highly cross-linked surface [19]. Eventually, alginate bead forms and the bioactive compounds are entrapped within the cross-linked matrices.

In the previous reports, the alginate-thyme essential oil (TEO) emulsions were extruded with a syringe into a calcium chloride bath. The result demonstrates that oil-loaded alginate beads [20] can be successfully prepared by external gelation method. The loading capacity of TEO in beads was higher than 50%. TEO-loaded alginate beads are to release TEO during the digestive process in animals, enhancing its antimicrobial effect. Moreover, many oil-loaded alginate beads were studied including the addition of other fillers to improve their properties. The sunflower oil (SO)-loaded alginate/shallac beads [21] fabricate by external gelation method. The loading capacity of SO in beads was 38%. SO-loaded alginate bead was further studied the *in vitro* digestion, the results showed more oil released during intestinal digestion than during gastric digestion. These findings have important for the design of delivery systems.

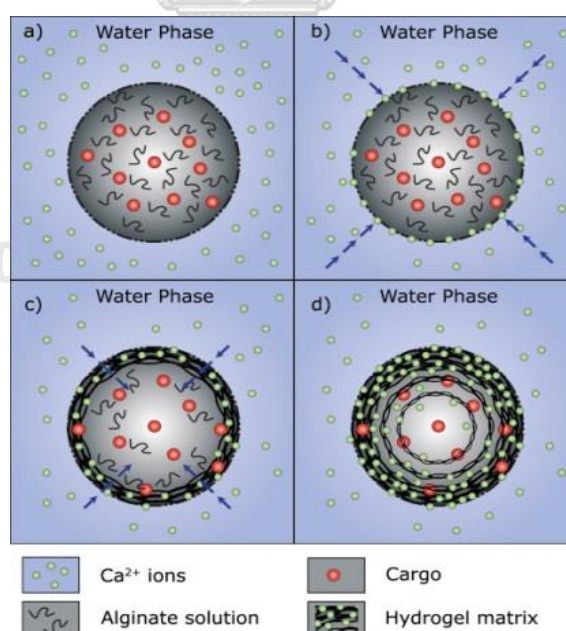


**Figure 2.3** Mechanism of external gelation for bead formation: (a) alginate droplet into a  $\text{Ca}^{2+}$  ions bath, (b) inward diffusion of calcium ions, (c) inward gelation of droplet, and (d) completed gelation [22].

### 2.1.2.2 Internal gelation

For internal gelation, the mixture of alginate solution, cargo and insoluble calcium salt ( $\text{CaCO}_3$ ) is extruded into oil bath containing acetic acid. Acetic acid renders the release of  $\text{Ca}^{2+}$  from  $\text{CaCO}_3$  leading to internal cross-linking in the alginate droplet (Fig. 2.4) [23]. In addition, carbon dioxide ( $\text{CO}_2$ ) is generated in the same time, resulted in creating the porous cross-linked alginate bead [19]. However, this kind of alginate bead has low loading capacity and the entrapped substances are faster released [24-26]. Moreover, the production of bead tended to coagulate large masses when speed up extrude, it is difficult in controlling the gelling conditions in the emulsion.

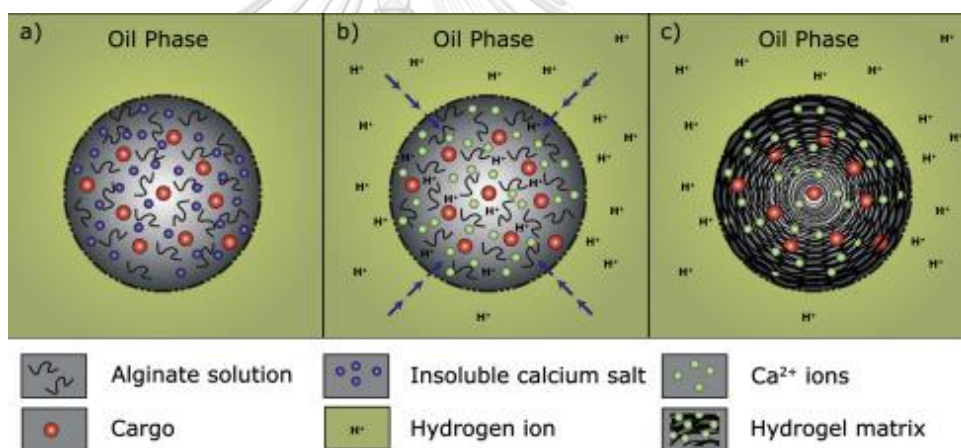


**Figure 2.4** Mechanism of internal gelation for bead formation: (a) dispersion of alginate droplet in oil, (b) addition of acid to dissolve the calcium salt, and (c) localized gelation of droplet [22].

### 2.1.2.3 Inverse gelation

In another gelation mechanism, an emulsion of oil containing  $\text{Ca}^{2+}$  ions and cargo is extruded into an alginate bath. When emulsion droplet contacts alginate solution, the  $\text{Ca}^{2+}$  ions diffuse to the outer boundary of the droplet and cross-link with the alginate polymer chains form membranes around (Fig. 2.5). The gelation process continues until the free  $\text{Ca}^{2+}$  ions are depleted. At the end of the process,

the initial emulsion droplet is encapsulated by alginate membrane. The alginate bead fabricated by inverse gelation method was previously used to encapsulate plant cells, bacteria, enzymes, and vegetable oils [27-29]. However, the alginate beads from this method are not usually spherical, they can easily be deformed upon impact with the surface of the alginate bath. The deformed bead is happened because alginate solution has a higher viscosity than the emulsion droplets. Moreover, several difficulties are inherent to this method. The primary, the weak alginate membrane formed by low alginate concentrations may cause the beads to easily break down. In another, the constant diffusion of free  $\text{Ca}^{2+}$  ions from the emulsion droplets leads to the difficult control of the gelation process and may cause agglomeration between beads of the entire alginate bath [30].

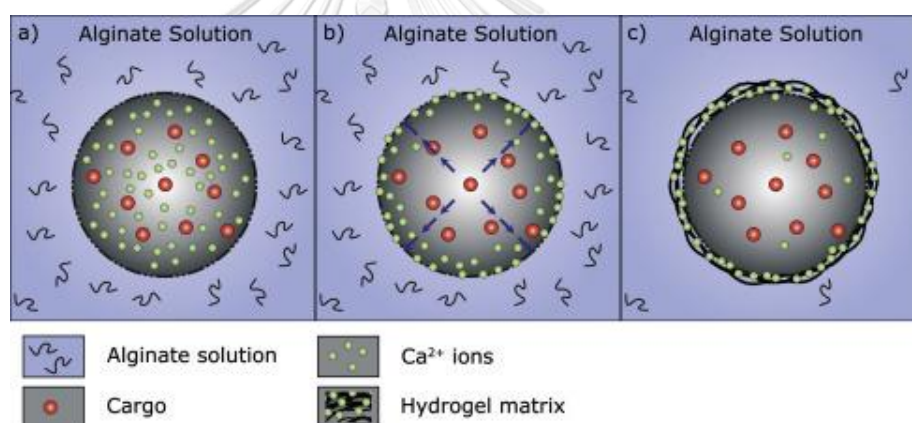


**Figure 2.5** Mechanism of inverse gelation for liquid-core capsule formation: (a) droplet containing calcium ions in contact with alginate solution, (b) outward diffusion of calcium ions, and (c) gelation at droplet interface [22].

From the above methods, it is obvious that the active compound has to mix with some substances before forming beads. Thus, its loading is quite low. Moreover, several difficulties are inherent to those methods that mentioned above.

## 2.2 Capsules

Capsules use as encapsulate for biomedical and pharmaceutical applications. The appearance of capsules was spherical or rods with common diameter of 1-10

mm, active compounds based core within the shell capsules comprise at least 80% by weight of the capsule. Unlike the beads encapsulated substances quite lower than capsules due to substances mixed with excipients or materials matrix. In addition, the diameter of beads is a ranging of 20-2000  $\mu\text{m}$ .

### 2.2.1 Commercial capsules

The two main types of capsules are hard capsules and soft capsules. The most commonly raw material used to make both types of capsules are gelatin. Gelatin is derived from collagen obtained from various parts of animals. The sources of the gelatin are pig skin (46%), bovine hides (29.4%), bones (23.1%) and other sources (1.5%) [31]. Gelatin has good mechanical properties and dissolves easily at a temperature close to human body. These properties make it being the best material for fabricating commercial capsules in nowadays.

#### 2.2.1.1 Hard capsule

Hard capsule [32] consists of two halves bodies which are a smaller-diameter body and a larger-diameter cap. Medicines or active ingredients (mostly solid) are filled in a small body and then sealed using a large cap (Fig. 2.6). The body and cap of capsule are normally rod-shaped gelatin.

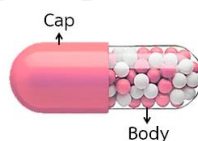


**Figure 2.6** Hard capsule is created of a two piece.

#### 2.2.1.2 Soft capsule

Soft capsule [33, 34] is suitable for oils and liquid active compounds. Soft capsule can mask unpleasant odors and tastes of filled substances. The manufacture soft capsules using the rotary die method [35] as shown in Fig. 2.7. A rotary die

machine has a pair of roller dies to guide the two gelatin sheets into contact with each other between two co-acting dies. The proper amount of filling active compound is simultaneously dispensing between the sheets in half-cavities on the outer surface of the dies. At the same time, the rotary die system cuts and hermetically seals the two half-cavities of the film sheet together.

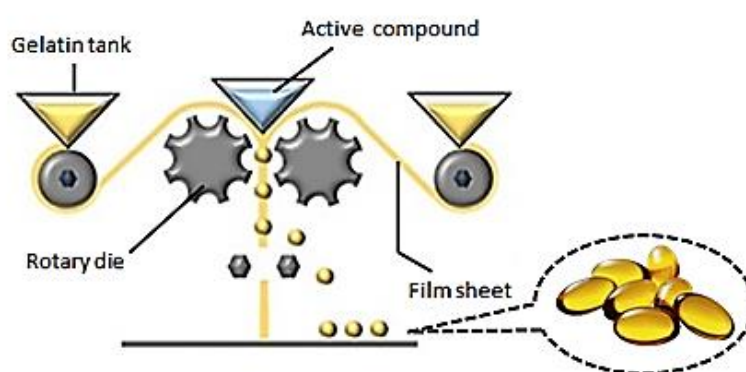


**Figure 2.7** Manufacture soft capsules using by the rotary die method [33].

At present, raw material for capsule production is gelatin. A number of factories produce the edible gelatin from waste pig skin due to low cost. Recently, the alternative gelatin sources are chicken and fishes (fish gelatin) but these could not fulfill various industries demand due to high costs. In addition, manufacturing of halal capsules is made from cattle bone and cattle hide gelatin, which are higher cost. However, the consumers are also concerned about the spread of diseases from animal sources of gelatin to human. For these reasons, the interesting alternative polymer sources are plants-derivative, which increasingly have more researches and development. One of them is the alginate extracted from algae.

### 2.2.2 Alginate capsule

Usually, alginate is used into form of beads to encapsulate a variety of substances in effectively. Furthermore, there has been a continuous research in the



development of processes and techniques able to fabricate alginate capsules for increasingly encapsulate of substances.

In 2013, Jun Wu and colleagues [8] fabricated poly(lactic-co-glycolic acid (PLGA)-alginate core-shell microspheres using capillary microfluidic devices (Fig. 2.8). Firstly, PLGA solution in dichloromethane (DCM) containing rifampicin, the alginate solution and toluene containing span 80, as the inner oil phase, middle aqueous phase and outer oil phase, respectively, were guided into the microfluidic device to generate PLGA–alginate droplets. Secondly, the emulsion droplets were incubated in calcium chloride solution to cross-link the alginate shell layer. Lastly, the hardened droplets were collected and left until complete evaporation of DCM at room temperature. The obtained PLGA–alginate microspheres were washed with distilled water and dried at 40 °C. The sizes of rifampicin-loaded PLGA cores were in a range of 15 to 50  $\mu\text{m}$  which were controlled by the geometries of microfluidic devices and the fluid flow rates. It was also found that increasing the size of the PLGA microspheres could increase the encapsulation efficiency. The addition of PLGA in alginate shell can reduce the initial burst release and also modulate the drug release.

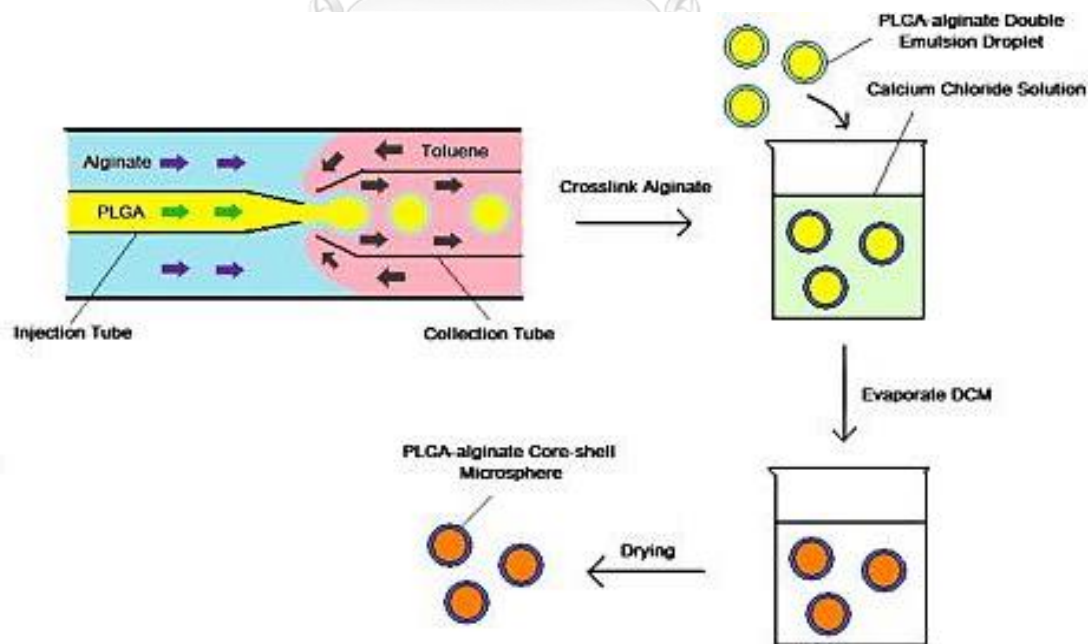


**Figure 2.8** Fabrication process of PLGA–alginate core–shell microspheres [8].

In 2014, Nittaya and colleagues [9] fabricated olive oil-loaded alginate macrocapsules using electro-coextrusion equipment quipped with a high voltage power supply (Fig. 2.9). The coaxial nozzle composed of an inner core tube (0.26 mm of inner diameter) and an outer shell tube (1.07 mm of inner diameter). The core and shell fluids were dropwised into 5% CaCl<sub>2</sub> solution. The effects of three factors in preparing olive oil-loaded alginate macrocapsules were studied, which were alginate concentration, alginate (shell) flow rate, and applied voltage. The diameter and shell thickness of macrocapsules were in the ranges of 0.89–1.61 mm and 17.4–66.4 μm, respectively. The higher alginate concentration resulted in the formation of larger and stronger macrocapsules with thicker shell. The increment of alginate flow rate increased the alginate amount in each droplet. This led to faster and tighter crosslink with Ca<sup>2+</sup>, resulting in the smaller capsule size but less desirable surface appearance. When the applied voltage increased, the droplet dripping frequency increased. The rapid dropping made the lessened surface tension, resulting in smaller and weaker capsules with thinner shell. The microscopic photographs of different types of macrocapsules were shown in Fig. 2.9.

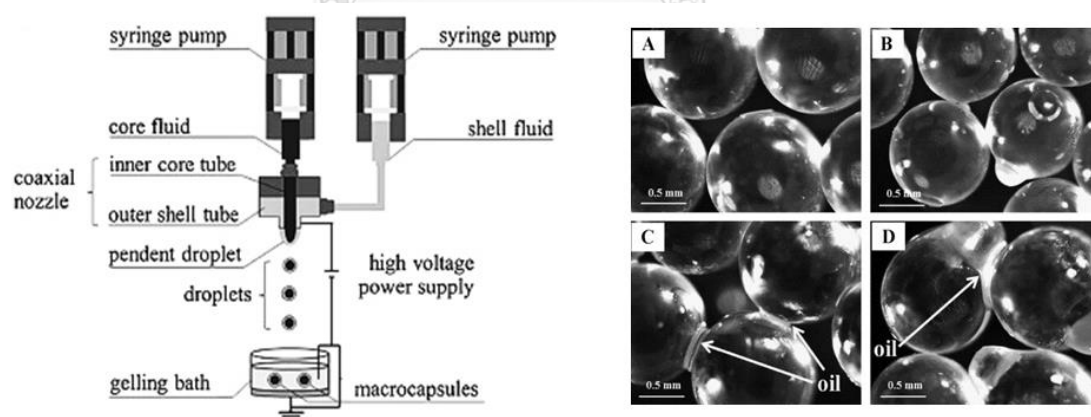


**Figure 2.9** Device of electro-coextrusion process for fabricated olive oil-loaded alginate macrocapsules (Left). photographs of the alginate macrocapsules different types of surface appearance (Right): (A) non-oily and smooth surface, (B) non-oily and rough surface, (C) oily and smooth surface, and (D) oily and rough surface [9].



In 2014, Pasquale and colleagues [10] manufactured alginate capsule through a prilling apparatus equipped with co-axial nozzles (Fig. 2.10). The core solution was piroxicam (PRX) suspended in pectin solution. The capsule was manufactured by a vibrating nozzle device by pumping alginate solution (outer) and PRX/pectin (inner) suspension through a co-axial nozzle system at 10 mL/min of flow rate and 350 Hz of vibration frequency. The droplets were gelled with zinc acetate solution. The capsules diameter was distribution in the range of 2131–2598  $\mu\text{m}$ . Results showed the satisfying encapsulation efficiency (E.E.) values of dried capsules which were 86.3%.

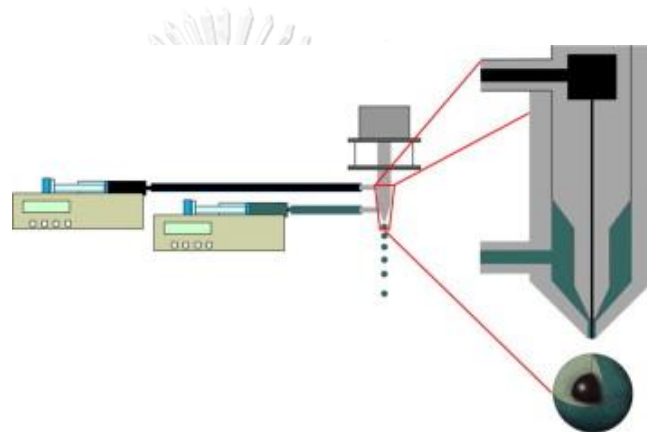


**Figure 2.10** The schematic illustration of the microencapsulation process to obtain core-shell particle structure by co-axial prilling [10].

In 2015, Meghdad and colleagues [11] used melt coaxial electro spray to produce microcapsules (Fig. 2.11). The shell of capsules made from sodium alginate which was loaded by an outer syringe. The core of them was n-nonadecane which was melted at 50 °C before injection by the inner syringe. The fabricated capsules were dripped into 2% calcium chloride bath. The effect of alginate concentration and working distance on microcapsule size was studied. It was found that the decrease of working distance from 20 to 5 cm led to decrease the capsules diameter from 480 to 275  $\mu\text{m}$ . In addition, the decreased of alginate concentration also decreased the capsules size.

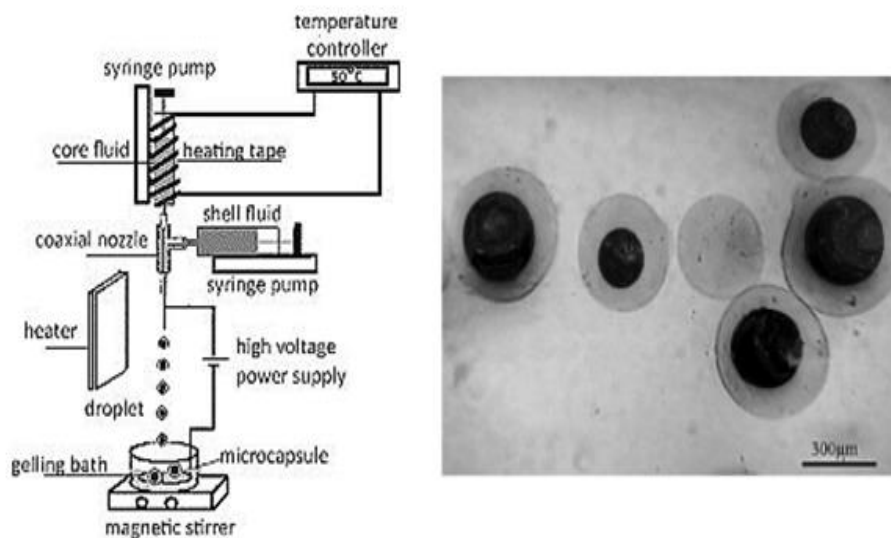


**Figure 2.11** Device of the melt coaxial electro-spray (Left), and photographs of the alginate macrocapsules (Right) [11].

In 2017, Danish and colleagues [36] reported a robust microfluidic platform for generating alginate microcapsules (Fig. 2.12). A combined co-axial flow and T-junction device were used to generate the microcapsules. The double emulsion droplets were produced by co-axial flow in which the silicone oil was core and alginate solution was shell. After that, the droplets were merged into the aqueous calcium chloride droplets which flowed out from a T-junction. The microcapsules diameter was in a range of 840-950 μm. However, the high viscosity of the alginate solution caused the tear drop shape, resulting in small tail-like particles after gelling and drying (Fig.2.12).

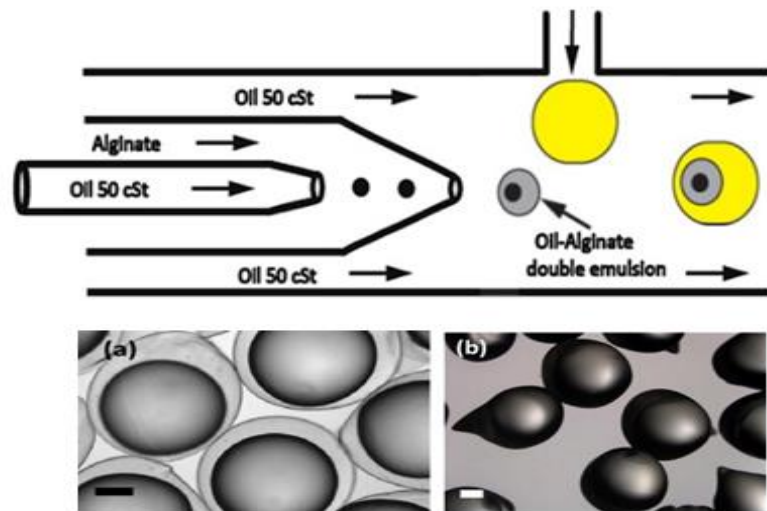


**Figure 2.12** Schematic of robust microfluidic platform for generating alginate microcapsules and Wet image of alginate microcapsules (a) and Dry image of alginate microcapsule (b) (Scale bar 200  $\mu\text{m}$ ) [36].

## 2.3 Bacterial Cellulose (BC)

### 2.3.1 Source and general properties

Bacterial or microbial cellulose (BC) known as *nata de coco* is synthesized by *Acetobacter*, *Agrobacterium*, *Alcaligenes*, *Pseudomonas*, *Rhizobium*, or *Sarcina sp.* [37]. BC composes of repeating units of the monomer,  $\beta$ -D-glucopyranose,  $-\text{[C}_6\text{H}_{10}\text{O}_5\text{]}-$ , covalently connected through  $\beta$ -1,4-glycosidic bonds (C–O–C) between the C4 and C1 carbon atoms as shown in Fig. 2.13 [38]. The individual chains are connected via hydrogen bonds and these are configuration of 1.5 nm sub-fibrils, 3.5 nm micro-fibrils and finally into flat ribbons that are 100 nm wide [39]. However, BC fibers are finer and higher purity without any hemicellulose or pectin than plant cellulose. BC has unique properties, such as high water-holding capacity [40], high crystallinity, fine fiber networks, and high tensile strength [41]. BC is used in a variety of applications in industry, consumer goods, medicine [42], and also used as environmentally-friendly polymeric material, which is now receiving more attention in nowadays.

In term of good mechanical property, BC has been studied as reinforcement agent in many composite materials. For examples, Suchata et al. (2015) prepared BC-alginate composite (BCA) [43] for using in the tissue engineering. BCA composites were cross-linked with calcium chloride. Tensile strength (TS) values of BCA composites with weight ratios of BC and alginate at 70:30 (12.16 MPa) were significantly higher than pure alginate films (0.87 MPa), which indicate that the BC can significantly enhance the mechanical property of alginate composite. Xuejiao et al. (2017) prepared bio-composite films, which mixing protein extracted from buckwheat with BC [44]. The film showed that BC is compatible with protein matrix and high rigidity. Tensile strength (TS) values of pure protein films and composite films (containing 2.0% BC) were 4.26 MPa and 15.03 MPa, the result showed BC can significantly increase the mechanical property of bio-composite films. Furthermore, Yuanyuan et al. (2017) prepared BC-chitosan composite [45] as scaffold bioactive materials. BC used as reinforcement for these materials including its cell proliferation and biocompatibility.

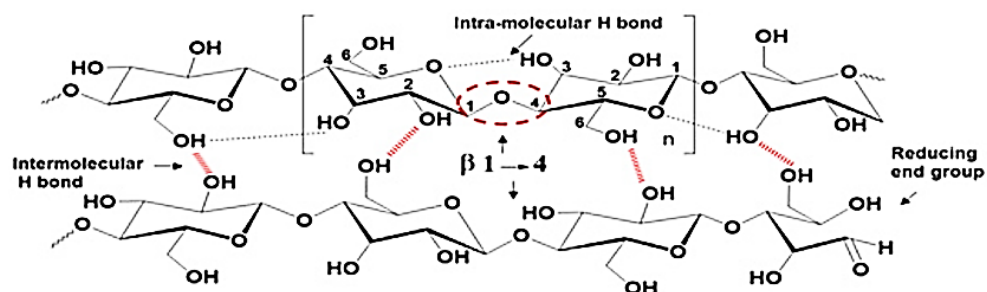


**Figure 2.13** The molecular structure of bacterial cellulose [38].

However, BC microfibrils are poorly distributed in aqueous state and polymer materials due to a large number of hydrogen bonds between its fibrous networks (Fig. 2.13) [46]. Thus, chemical modification of hydroxyl groups on BC surface can solve this problem. Among of them, oxidation using 2,2,6,6-tetramethyl-1-piperidine-N-oxy radical (TEMPO) has been one of the most potential promising methods for cellulose functionalization.

### 2.3.2 TEMPO-oxidized cellulose

The hydroxyl group on cellulose surface can be easily oxidized by 2,2,6,6-tetramethyl-1-piperidine-N-oxy radical (TEMPO) to be carboxylate groups [46-48] (Fig. 2.14). The carboxyl groups on the surface of TEMPO-oxidized cellulose increased the gaps between adjacent fibers as a result of the repulsive inter-action of anionic charges, which resulted in a well-aqueous dispersed state [46, 49]. This method is mild and environmentally friendly conditions and produces oxidized yields of up to 90%.

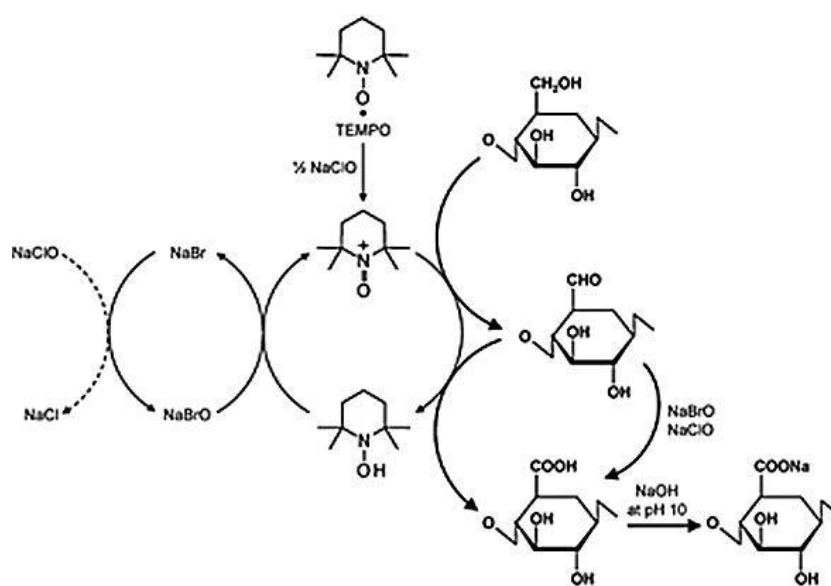


**Figure 2.14** TEMPO-mediated oxidation process of bacterial cellulose [50].

In the previous reports, TEMPO-oxidized cellulose was used as for improving the mechanical property of many materials such as hydrogel, scaffold and sponges.

In 2012, Ning Lin and colleagues [51] prepared TEMPO-Oxidized cellulose reinforcing in the alginate-based sponges. TEMPO-Oxidized cellulose contains the same carboxyl groups as alginate, and they both participate in the  $\text{Ca}^{2+}$  crosslinking process. TEMPO-Oxidized cellulose can not only participate to the crosslinking but also is involved with alginate in the structural construction of the sponges, which can form a semi-interpenetrating polymer network (SIPN) in ensuing alginate-based sponges (Fig. 2.15). Furthermore, the mechanical testing of the  $\text{Ca}^{2+}$  crosslinked

sponges indicated that alginate-based sponges filled with oxidized cellulose were generally stronger and more robust than neat alginate.

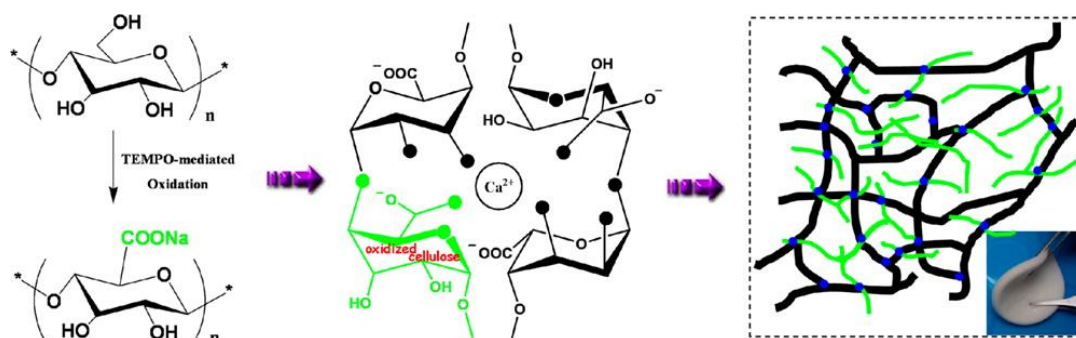


**Figure 2.15** Schematic representation of the structure of egg-box junction zones in TEMPO-mediated oxidation of cellulose/alginate/calcium system [51].

In 2017, Xiao-jun and colleagues [52] prepared alginate reinforced with TEMPO-oxidized cellulose in composite fibers. The incorporation of oxidized cellulose increased the opacity of the spinning dopes but improved the mechanical properties of the alginate fibers. The optimum addition amount for all of the oxidized cellulose was 5% (based on the weight of alginate). All the composite fibers had an irregular cross-section with dense and uniform structure, which indicated the good compatibility between oxidized cellulose and alginate. In addition, the introduction of oxidized cellulose slightly improved the thermal stability of the alginate fibers.

In 2017, Ragab and colleagues [53] produced scaffolds for bone tissue engineering by extrusion-based 3D printing technique. They prepared TEMPO-oxidized cellulose nanofibril (T-CNF)/alginate (SA) hydrogel through partial cross-linking (Ca<sup>2+</sup>) for printing the hydrogel. The hydrogel with 2% T-CNF nanofibril and 2% SA hydrogel displayed the highest fidelity in the reproduction of the digital object and the best printability. The compressive strength was increased from 87 to 455 MPa for pure T-CNF and T-CNF/SA, respectively. T-CNF/SA scaffolds exhibited excellent mechanical properties compared to pure SA and pure T-CNF.

The TEMPO-oxidized cellulose used as reinforcing agents which have reported in many studies. However, alginate capsules with TEMPO-oxidized bacterial cellulose (TOBC) additive have not been reported.



## CHAPTER III

### EXPERIMENTAL

#### 3.1 Chemicals and materials

Sodium alginate was purchased from Union Chemical 1986 Co., Ltd. (Thailand). Calcium chloride ( $\text{CaCl}_2$ ), sodium bromide (NaBr), sodium hypochlorite (NaClO) and (2,2,6,6-tetramethylpiperidin-1-yl)oxyl (TEMPO) were purchased from Sigma-Aldrich (USA). BC pellicles (nata de coco) were obtained from a local market in Chonburi, Thailand. Glycerol (99% purify) was supplied by Virotevitayapun Company, Thailand.

#### 3.2 Preparation of TEMPO-oxidized bacterial cellulose (TOBC)

BC pellicles were treated in 0.5 M NaOH solution at 90 °C for 2 h and then soaked in acetic acid solution for neutralization and washed with deionized water. Then, the treated BC was minced by a blender, filtered and freeze-dried. The freeze-dried BC was oxidized using a TEMPO-mediated system. Firstly, 1 g of dried BC was minced and suspended in 100 mL of distilled water containing 0.1 mmol of TEMPO and 1 mmol of NaBr. The oxidation reaction was started by dropping 15 mL of NaClO under continued stirring at ambient temperature for 5 h. The oxidation was quenched by adding ethanol to the suspension until the solution color change. The reaction product was centrifuged at 6000 rpm for 10 min. The supernatant was removed, and the precipitate was cleaned repeatedly with deionized water. The TOBC was obtained after freeze-drying for further experiments.

#### 3.3 Characterization of TEMPO-oxidized bacterial cellulose (TOBC)

##### 3.3.1 Attenuated total reflection fourier transform infrared (ATR-FTIR) spectroscopy

The functional groups of TOBC were investigated using attenuated total reflection fourier transform infrared (ATR-FTIR) spectroscopy. FTIR spectra were



recorded using a PerkinElmer Spectrum 100 spectrophotometer. Spectral width ranging from 4000 to 800  $\text{cm}^{-1}$  with 4  $\text{cm}^{-1}$  resolutions and an accumulation of 16 scans.

### 3.3.2 Determination degree of oxidation

The carboxylate content of TOBC sample was determined by electric conductivity titration method. The 2 mL of 0.05 M NaCl was adding in 30 mL of TOBC (0.1 wt%). The pH was maintained at 3 by the addition of 0.1 M HCl in order to protonate the carboxylate groups. The solution was titrated against 0.1 M NaOH in 0.1 mL increments. The degree of oxidation was determined by the following equation 1.

$$\text{Degree of oxidation} = \frac{162 \times C \times (V1 - V2)}{m - 36 \times C \times (V1 - V2)} \quad (\text{eq. 1})$$

Where  $C$  is the concentration of NaOH (mol/L),  $V1$  and  $V2$  are the first and second equivalent volumes of NaOH which are obtained from the plateau (L) of titration graph. And  $m$  is the mass of the TOBC (g).

### 3.3.3 X-ray diffraction (XRD) analysis

X-ray diffraction spectra of the BC and TOBC were obtained using a Rigaku ULTIMA IV X-ray diffractometer, using K. The diffracted intensities for each sample were recorded from  $10^\circ$ – $30^\circ$  at  $2\theta$  angles. The sample were distributed in holder and the instrument operating at a scanning rate of 0.5/min, using a voltage of 36 kV and a current of 20 mA. The data were obtained with the help of an MDI/JADE6 software package attached to the Rigaku XRD instrument. The Crystallinity (%) = (total area of crystal diffraction/total area of crystal and amorphous diffraction)  $\times$  100% [54].

## 3.4 Preparation of rice bran oil loaded alginate capsules

Alginate solution was prepared by firstly mixing alginate and TOBC in deionized water. The various TOBC contents; 0, 0.12, 0.25, 0.50, and 0.75 %w/v in alginate solution 1 %w/v, were studied. These solutions were dissolved under

continuous magnetic stirring at room temperature to achieve a turbid solution. Glycerol (5%v/v) was added in the solution and subsequently this solution was homogenized at 5000 rpm for 10 minutes. The alginate capsule device was shown in Fig. 3.1. The alginate solution and rice bran oil, which were core and shell substances, respectively, were loaded in syringes No.1 and 2, respectively. The distance between the glass tube tip and the CaCl<sub>2</sub> bath was 5, 10 and 20 cm, respectively. The flow rate of core and shell substances was controlled by syringe pump (Model LSP01-1A, Longer Precision Pump Co., Ltd). The inner and outer diameters of glass tube tip were 4 and 6 mm, respectively. From the preliminary test, the appropriate flow rate of core and shell substance was 5 and 16 mL/min, respectively. With these flow rates, it was founded that the core and shell substances fall from the tip together and gotten the complete capsule. The fabricated capsules were incubated in 2% w/v calcium chloride solution under magnetic stirring for 10 minutes. Then capsules were taken out and washed with distilled water three times. Capsules were allowed to dry at 50 °C for 10 hours. The capsule formation efficiency (%CFE) was obtained using equation 3.

$$\text{Capsule formation efficiency (\%CFE)} = \frac{\text{Number of oil loaded capsules (30s)}}{\text{Number of total drops (30s)}} \times 100 \quad (\text{eq.3})$$

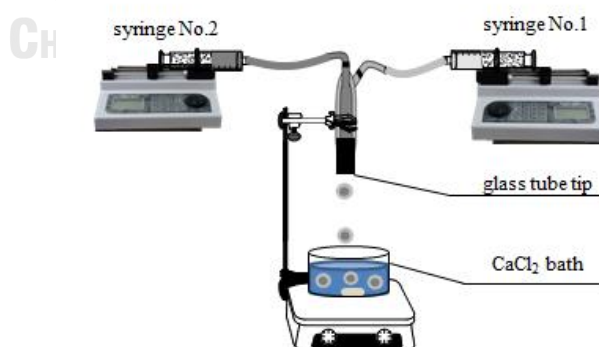


**Figure 3.1** Device for the fabricated alginate capsules.

### 3.5 Characterization of rice bran oil loaded alginate (OA) capsules

#### 3.5.1 Surface appearance, size, and thickness

The surface appearance of capsules was observed with digital camera at a magnification of x40. Size of capsule was determined with a digital electronic vernier caliper micrometer (Mituto, Tokyo, Japan). Thickness was measured by cutting a half of freeze-capsule and the thickness of shell was determined using a digital thickness gauge (SHAHE, Chengdu city, China). Size and thickness were measured at least ten random capsules and results reported as mean and standard deviation.

#### 3.5.2 Mechanical property

The mechanical property of alginate capsules was studied using a TA-XT2i (icon) Texture Analyzer (Stable Micro Systems, England). The instrument is equipped with a 50 N load cell fitted with a TA-P/5 separating rod fixture. The P/5 has short rods of 5 mm diameter each, protruding horizontally from the fixture. The starting position for the two rods is 5 mm apart. The alginate capsules are mounted onto the pair of rods. The probe moves downwards at a speed of 1 mm/sec until the capsules are chapped. The applied force is recorded as a function of distance.

### 3.6 Preparation of TOBC-alginate films

TOBC-alginate film solution was prepared using the same composition as solution for alginate capsules. After solution homogenization, the solution was chilled at 4 °C for overnight to remove air bubbles. The solution (90 g) was poured in a polystyrene petri disc (15 cm diameter) and dried in an oven at 50 °C for 18 h. Then material was successively soaked in 2 wt% CaCl<sub>2</sub> solution for 10 minutes, rinsed and washed with deionized water. The cross-linked film was further oven-dried at 50 °C for 6 h. Films were preconditioned for at least 48 h in a constant temperature and humidity chamber (25 °C and 50% relative humidity (RH)) to ensure the stabilization of their water content before further characterization.

### 3.7 Characterization of TOBC-alginate films

#### 3.7.1 Thickness

Thickness (mm) of films was measured using a digital thickness gauge (SHAHE, Chengdu city, China). Each film sheet was measured at different points at least five random locations and results reported as average values and standard deviation.

#### 3.7.2 Light transmission and transparency

The ultraviolet and visible light barrier properties of the films were analyzed in a spectrophotometer using transmittance mode. The films were placed directly into the spectrophotometer cell according to the method described by Fang et al. [55]. Film transparency was determined by the ratio between the transmittance at 600 nm ( $T_{600}$ ) and calculated by the following equation 4.

$$\text{Transparency value} = -\log T_{600}/b \quad (\text{eq. 4})$$

Where  $T_{600}$  is the fractional transmittance at 600 nm and  $b$  is the film thickness (mm). The film thickness was done in triplicate. The greater value represents lower transparency of the film.

#### 3.7.3 Thermal gravimetric analysis (TGA)

The thermogravimetric characteristic of composite film was measured by TGA (SDTA851e, Mettler Toledo, Columbus, USA). This technique was used to determine the onset temperature of overall thermal degradation ( $T_{deg}$ ) of samples. The samples were heated from 30 to 600 °C at the rate of 10 °C/min with nitrogen gas purged at 30 mL/min.

#### 3.7.4 Scanning electron microscopy (SEM) analysis

The surface morphology of the films was observed at an acceleration voltage of 5 kV using scanning electron microscopy (SEM, JSM-6480LV, JEOL, Japan). Before visualization, the samples were mounted on the metal stub, using double sided

adhesive tape then coated with a thin gold layer under vacuum to make them conductive. SEM images were taken at a 90° angle to observe the film surface.

### **3.7.5 Attenuated total reflection fourier transform infrared (ATR-FTIR) spectroscopy**

The structural interaction of blending in alginate-TOBC films was observed with a Nicolet 6700 fourier transform infrared (FTIR) spectroscope (Thermo Electron Scientific, Madison, WI) using the attenuated total reflection (ATR) method. The spectrum was measured using an automatic signal over 16 scans in the range of 800–4000  $\text{cm}^{-1}$  at a resolution of 4  $\text{cm}^{-1}$ , and the data were controlled against a background spectrum.

### **3.7.6 X-ray diffraction (XRD) analysis**

X-ray diffraction spectra of the BC and TOBC were obtained using a Rigaku ULTIMA IV X-ray diffractometer, using K. The diffracted intensities for each sample were recorded from 10°–35° at 2 $\theta$  angles. The films sample were cover on holder and the instrument operating at a scanning rate of 0.5/min, using a voltage of 36 kV and a current of 20 mA.

### **3.7.7 Mechanical property**

The mechanical property of the films was measured using a universal testing machine (UTMH10KM) with a 25 N load cell. All tests were carried out according to ASTM D882 standards and at least five specimens were tested for each condition. The films were cut into 80 mm×10 mm portions and left to stand at 30 °C and 35±5% relative humidity (RH) for 24 h prior to analysis. Each film specimen was mounted between the grips. The initial separation distance between the grips was set at 5 mm and the cross-head speed was 50 mm/min. Tensile stress (TS, MPa) and young's modulus (Y, MPa) were calculated using software.

### 3.7.8 Water vapor transmission rate (WVTR)

The Water vapor transmission rate (WVTR) was determined gravimetrically using a modified ASTM method E96–00 (ASTM, 1995) [56]. Glass bottle, with an average diameter of 5 cm were utilized to determine the WVP of the films. Initially, films were cut into circle with a diameter slightly larger than the diameter of the bottle. Approximately 20.0 g of desiccant was placed in each bottle and sealed with TOBC-alginate films using glue and paraffin film to maintain the RH at 0% in the bottles. All bottles were placed in a desiccator at a RH of 98% in the desiccator. Bottles were weighed every day for 7 days. The amount of water that permeated through the film was determined based on the weight that was gained in the bottles throughout the time frame of measurements. Tests were conducted in triplicate for each sample and water vapor transmission rate was calculated by the following equation 5.

$$\text{WVTR} = \frac{\Delta W}{At} \quad (\text{eq. 5})$$

Where  $\Delta W$  is the weight of water permeating through the film (g);  $A$  is the permeation area ( $\text{cm}^2$ );  $t$  is the permeation time (Day).

### 3.7.9 Oxygen transmission rate (OTR)

Oxygen transmission rate of TOBC-alginate films was analyzed on a MOCON OX-TRAN model 2/21 MH MODULE (Minneapolis, Minnesota, USA) apparatus equipped with a coulox sensor. Samples were placed in a specimen area of  $50 \text{ cm}^2$ . The ASTM standards that were used include D3985-17. The film was exposed to 99.7% oxygen. The measurements were carried out in duplicate at  $23 \text{ }^\circ\text{C}$ , 0% RH. Tests were conducted in triplicate for each sample.

### 3.10 Statistical Analysis

Quantitative data were reported as means  $\pm$  standard deviations, where indicated. Statistical analysis was performed using a one-way ANOVA analysis, followed by the Turkeys HSD for multiple comparisons. A  $p$ -value  $<0.05$  was considered statistically significant.

## CHAPTER IV

### RESULTS AND DISCUSSION

#### 4.1 Characterization of TEMPO-oxidized bacterial cellulose (TOBC)

##### 4.1.1 FTIR analysis and determination degree of oxidation

In this study, TEMPO-mediated oxidation is a process to produce carboxylate groups on BC surfaces. The primary OH group at C6 of glucose unit is converted to acid sodium salts under the condition as shown in Fig.4.1 to afford TOBC. The presence of asymmetric  $\text{-C=O}$  stretching band at  $1605\text{ cm}^{-1}$  in the FTIR spectra of TOBC (Fig.4.2a) proved the existence of carboxyl groups. Moreover, the stretching vibration band of the C-H at  $2890\text{ cm}^{-1}$  and stretching vibration band of the O-H groups near  $3339\text{ cm}^{-1}$  were slightly reduced after the modification in TOBC. The degree of oxidation (DO) or total amount of carboxyl groups can be determined by a conductometric titration. Typical titration curve of TOBC was shown in Appendix A. The value of  $\text{DO}_{(\text{TOBC})}$  calculated using eq.1 was 0.15.

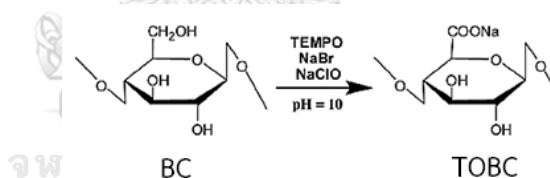


**Figure 4.1** The process to produce carboxylate groups on BC surfaces by TEMPO-mediated oxidation.

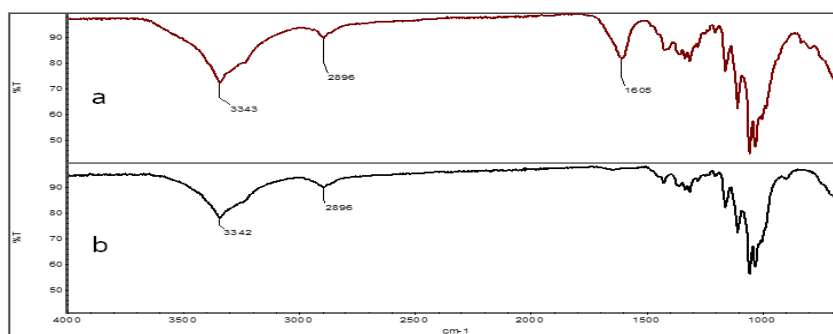


**Figure 4.2** FTIR spectra of TOBC (a) and BC (b).

#### 4.1.2 X-ray diffraction (XRD) analysis

The effect of oxidation on the crystalline structure of BC was further investigated with XRD analysis. After the modification the X-ray diffraction patterns were unchanged. TOBC and BC showed the diffraction peaks at  $2\theta$  angles located at  $14^\circ$ ,  $17^\circ$ , and  $22^\circ$  (Fig, 4.3). Meanwhile, the crystallinity of the TOBC was decreased from BC due to carboxyl groups on the TOBC that caused the repulsive interaction of anionic charges between adjacent fibers and resulted the increased amorphous and well-aqueous dispersion (Fig, 4.4).

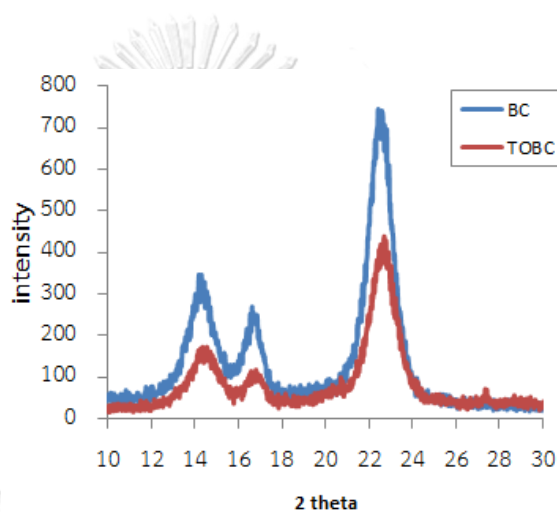


Figure 4.3 The XRD patterns of BC and TOBC.



Figure 4.4 Aqueous dispersion states of BC and TOBC.

### 4.2 Characterization of rice bran oil loaded alginate (OA) capsules

#### 4.2.1 Capsule formation efficiency (%CFE)

Rice bran oil-loaded alginate capsules (OA) were successfully fabricated using a coaxial-glass tube. The capsule formation efficiency (%CFE) was obtained using eq.



3 in Section 3.4. AT0, AT0.12, AT0.25, AT0.50 and AT0.75 were labeled for 0, 0.12, 0.25, 0.50 and 0.75 %w/v of TOBC in the 1 %w/v alginate solution, respectively. All alginate concentrations were dropped by difference distance between tube tip and the  $\text{Ca}^{2+}$  ions bath. The results shown in Fig. 4.5 indicated that the 5 and 10 cm gaps were given the higher %CFE than 20 cm gap. At the same gap, the increasing amount of TOBC led to increase the viscosity of shell solution, and resulting in the decreasing of %CFE. In this work, OA capsules were fabricated using extrusion-dropping technique, which capsule formation depended on the gravitational force and the viscosity of core and shell solutions. In this study, we controlled the droplet rate (drops/min) of the core and shell solutions to be almost similarity. However, the core and shell velocity of droplet of the core and shell solution was often different due to the viscosity and density. While droplets of the core and shell solution was dropped from tube tip to  $\text{Ca}^{2+}$  ions bath with different velocity led to fail capsule or core separate from shell droplet before cross-link by  $\text{Ca}^{2+}$ . Therefore, the less distance reduces this problem, so it had a high %CFE.

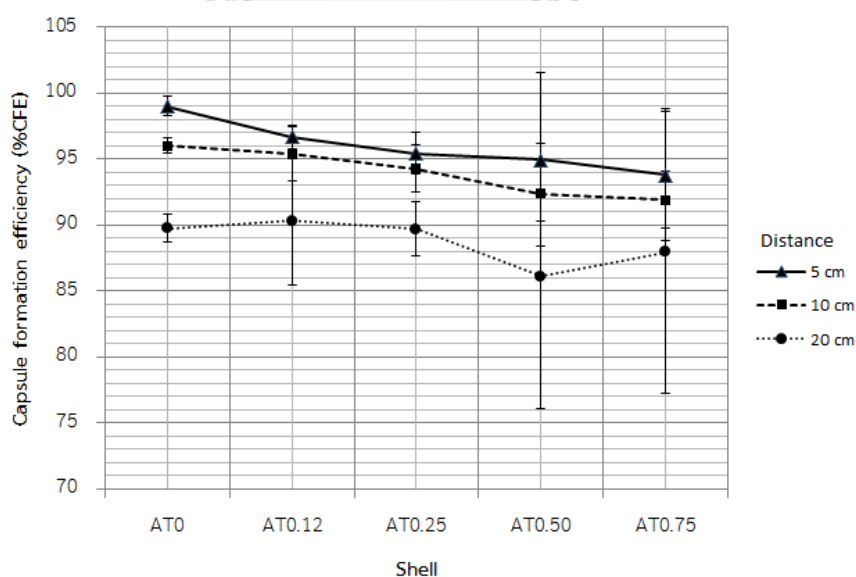


**Figure 4.5** Capsule formation efficiency (%CFE) of OA capsules.

#### 4.2.2 Surface appearance, capsule size, and shell thickness

The surface appearance of OA capsules was observed with digital camera at a magnification of 40X (Fig. 4.6). The surface of AT0-capsule shell was rough and transparent whereas AT0.12- and AT0.25-capsule shells were smoother and more transparent. The surface of capsules containing TOBC more than 0.50% was smooth but obviously turbid. The G blocks of alginate strongly cross-linked with  $\text{Ca}^{2+}$  ion which made the capsule surface being rough after drying. The carboxylate groups of TOBC can also weakly participate with the  $\text{Ca}^{2+}$  ion. Moreover, TOBC is involved in the structural construction of the capsule shell which protects the shrinkage of capsule surface [51, 57]. Thus, capsule containing TOBC had smooth surface but it also increased the turbidity.

The tail-like capsules were observed such as AT0.25-capsule at the 5 cm gap. The gap between tube tip and the  $\text{Ca}^{2+}$  ions bath, and viscosity of shell solution were the important factors on shape of capsule. The high viscosity of shell solution needs the higher gap to reduce formation of small tail-like capsules. In contrast, the lower viscosity desires shorter gap [58].

The average size and shell thickness of all capsules were shown in Table 4.1. The size was in a range of 4.18-4.59 mm which the maximum size difference was 9.8%. Figure 4.7a is the image of fresh capsules in which shell is colorless and core is blue. After drying, the shell was hardly observed by naked-eyes (Fig. 4.7b). We froze the capsule using dry ice and cut at half of capsule to measure the thickness (Fig. 4.7c). The thickness of most capsules was similarity. Thus, we concluded that the size and shell thickness were not depend on the gap and viscosity.

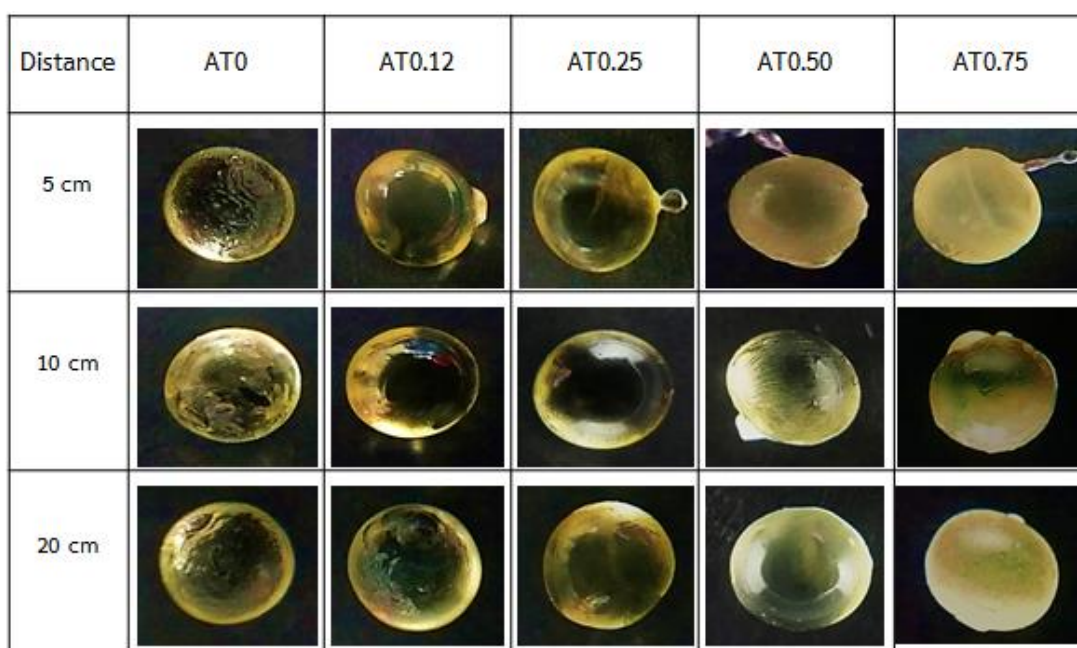


**Figure 4.6** Macroscopic capsules images of alginate with various TOBC contents and distance between tip tube and  $\text{Ca}^{2+}$  bath.

**Table 4.1** The size and thickness of capsules fabricated at different alginate shell solution and varied distances.

Capsules	Dry capsules size (mm) at difference gap			Thickness (mm) at difference gap		
	5 cm	10 cm	20 cm	5 cm	10 cm	20 cm
	AT0	4.30 ± 0.20	4.24 ± 0.33	4.21 ± 0.20	0.32 ± 0.10	0.31 ± 0.05
AT0.12	4.18 ± 0.13	4.19 ± 0.16	4.27 ± 0.32	0.34 ± 0.09	0.30 ± 0.13	0.33 ± 0.08
AT0.25	4.38 ± 0.12	4.28 ± 0.15	4.33 ± 0.09	0.31 ± 0.09	0.29 ± 0.18	0.31 ± 0.16
AT0.50	4.47 ± 0.21	4.38 ± 0.12	4.31 ± 0.14	0.31 ± 0.07	0.33 ± 0.07	0.33 ± 0.11
AT0.75	4.46 ± 0.31	4.46 ± 0.20	4.59 ± 0.23	0.35 ± 0.13	0.33 ± 0.03	0.34 ± 0.16

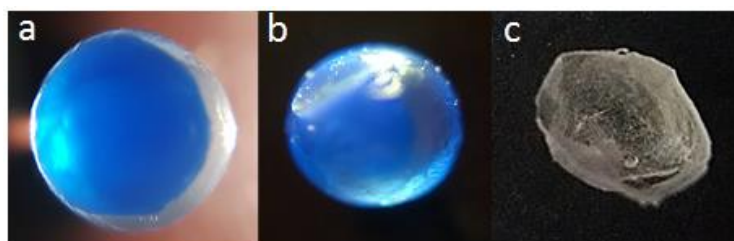


**Figure 4.7** Images of fresh (a) and dry capsules (b), and dried-shell without core (c).

#### 4.2.3 Mechanical property

The OA capsules which produced at 10 cm gap were selected for compression mechanical analysis. As expected, the compression strength of the OA capsules increased if the TOBC content increased (Fig. 4.8). However, 0.12 and 0.25% of TOBC did not improve the strength since they showed the same strength level as 0% of TOBC. At least 0.50% of TOBC significantly enhanced compression strength of capsules. This result confirmed that TOBC could participate in the crosslinking reaction and cooperate well with alginate to act as a structural and reinforcing agent.

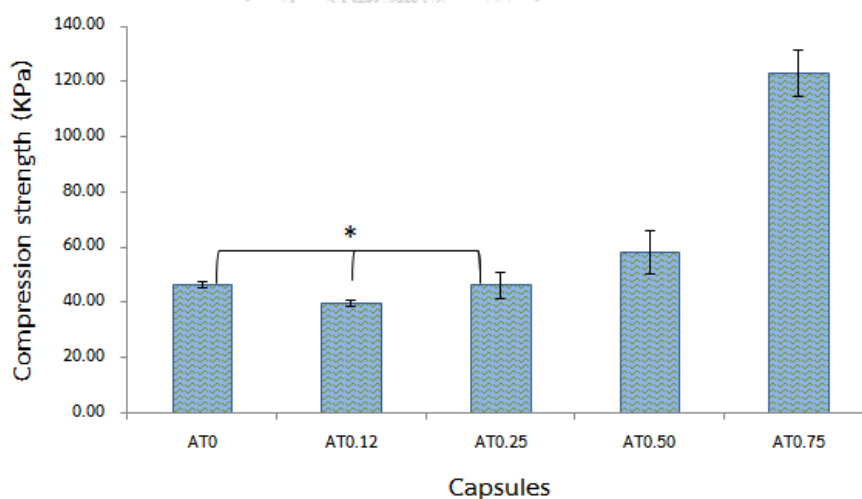


**Figure 4.8** The compression mechanical properties of the OA capsules.

\* Different superscripts within a chart indicate significant differences ( $p < 0.05$ )

### 4.3 Characterization of TOBC-alginate films

#### 4.3.1 Thickness, transparency and mechanical property

The TOBC-alginate film was used for characterization of shell properties. We try to fabricate film with the nearly the thickness median of capsule shell (0.32 mm) and use the same process as capsule preparation. Films were prepared by solvent casting method and ionic cross-linked by  $\text{Ca}^{2+}$  ion. The film thickness was in a range of 0.28-0.33 mm in which the increasing TOBC content slightly affected the thickness (Table 4.2).

The transmittance percentages of all films are presented in Appendix B. TOBC-alginate film transparency was calculated by the following equation 4 in section 3 and shown in Table 4.2. The greater value represents lower transparency of the film. The result indicated that the increase of TOBC content enhanced the film turbidity which was relative to the camera images in Fig. 4.9.

The mechanical properties of the TOBC-alginate films are influenced on the amount of TOBC incorporation. The stress/strain curves of all films were shown in Appendix C. The tensile strength and Young's modulus of alginate film without TOBC were 3.20 and 4.65 MPa (Table. 4.2), respectively. With the increment of TOBC content, both the tensile strength and Young's Modulus of the TOBC-alginate films were increased. Especially, AT0.50 and AT0.75 films exhibited the significant enhancement of Young's modulus. These changes in mechanical properties are consistent with the observed microstructures from morphology and XRD results (in Section 4.3.2). The mechanical improvement might be ascribed to the good interfacial interaction and compatibility between the TOBC and alginate matrix.

**Table 4.2** Thickness, transparency, tensile strength and Young's modulus of TOBC-alginate films.

films	Thickness (mm)	Transparency value	Tensile strength (MPa)	Young's modulus (MPa)
AT0	0.31 <sup>*</sup> ± 0.04	1.09 ± 0.03	3.20 ± 0.66	4.65 ± 0.41
AT0.12	0.28 <sup>*</sup> ± 0.03	2.04 ± 0.05	16.44 ± 1.38	21.41 ± 8.02
AT0.25	0.29 <sup>*</sup> ± 0.04	4.53 ± 0.08	18.81 ± 2.81	24.43 ± 3.56
AT0.50	0.32 <sup>*</sup> ± 0.02	5.32 ± 0.41	22.05 ± 1.09	60.87 ± 9.14
AT0.75	0.33 <sup>*</sup> ± 0.03	5.66 ± 0.22	27.26 ± 3.50	338.00 ± 24.97

\* Different superscripts within a chart indicate significant differences ( $p < 0.05$ )

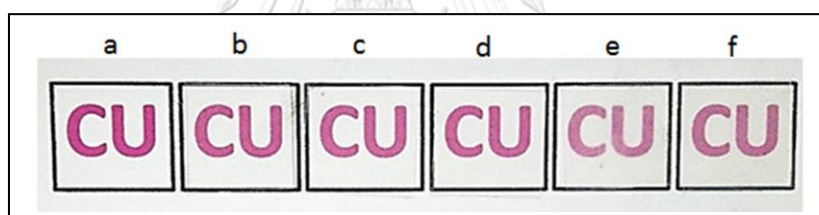


**Figure 4.9** The transparency of TOBC-alginate films; no film (a), AT0 (b), AT0.12 (c), AT0.25 (d), AT0.50 (e), and AT0.75 (f) (film samples).

#### 4.3.2 Morphology and X-ray diffraction (XRD) analysis

The camera images of films shown in Fig. 4.10A displayed that the TOBC addition decreased the shrinkage of films. This result was in agreement with that of capsules in Section 4.2.2. The carboxyl group of TOBC can participate in the  $\text{Ca}^{2+}$  crosslinking and also form a semi-interpenetrating polymer network (SIPN) in ensuing alginate-based films [R]. Moreover, the surface morphology of films observed by SEM was revealed that the surface was smoother when the amount of TOBC increased (Fig.4.10B). The cross-section of films showed the arrangement of film matrix (Fig. 4.10C). The film matrix of AT0-0.25 films shrunk in disorder pattern

whereas that of AT0.5-0.75 films showed mostly horizontal arrangement. This result was in agreement with the increase of crystallinity determined by X-ray diffraction (XRD) spectroscopy (Fig. 4.10D). This might be the addition of hydrogen bonding between the hydroxyl groups on TOBC and carboxyl groups on alginate chain. These results supported the effectiveness of TOBC in improving the mechanical property of alginate films.

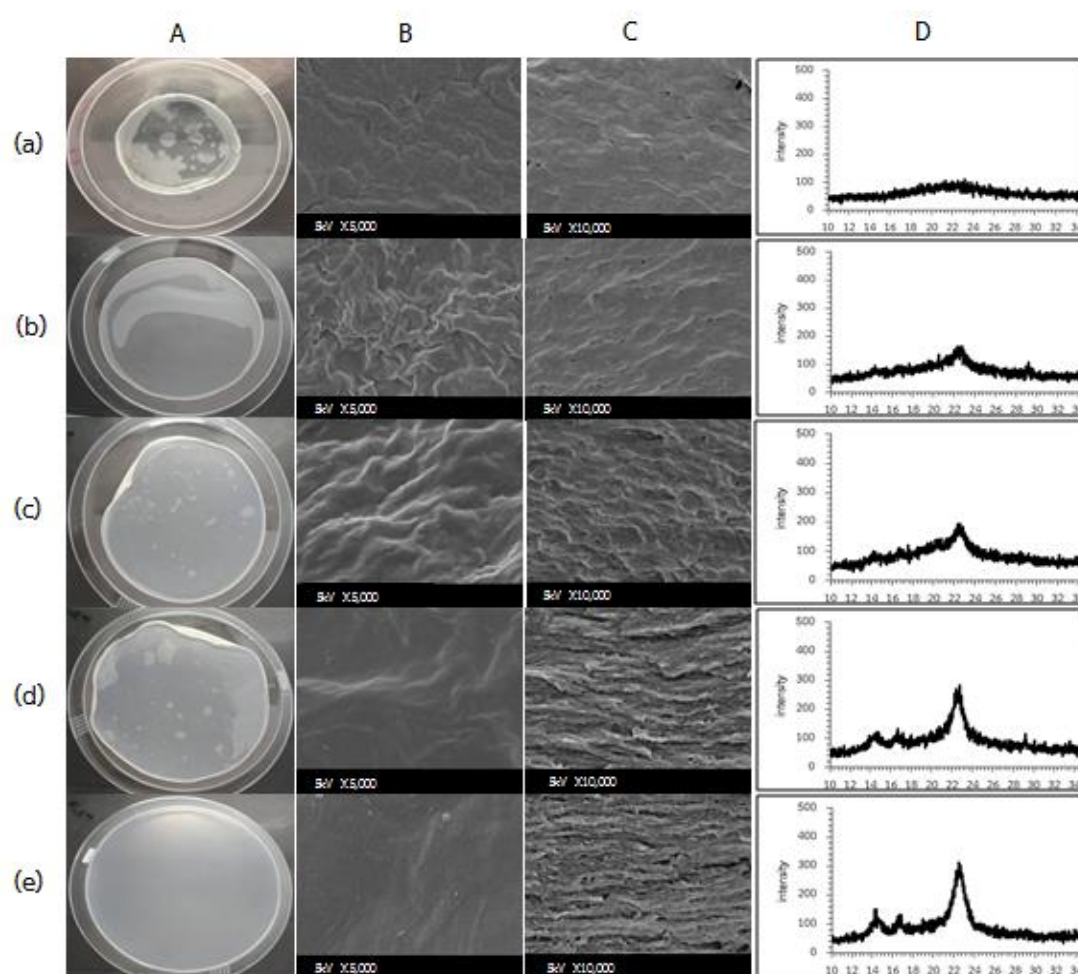


**Figure 4.10** Optical photos (A), SEM images (x5000) of surface morphology (B) Cross-section (x10000) (C), and XRD patterns (D) of alginate films contain 0% (a), 0.12% (b), 0.25% (c), 0.50% (d), and 0.75%w/v (e) of TOBC in 1%w/v alginate solution.

### 4.3.3 FTIR analysis

The FT-IR spectra of the films and TOBC were shown in Fig. 4.11. The spectra of both alginate film and TOBC displayed the major characteristic peaks similar. The



peak of the carbonyl ( $\text{—C=O}$ ) group of alginate film and TOBC which is located at  $1602$  and  $1605\text{ cm}^{-1}$ , respectively. The TOBC-alginate films which containing low TOBC content showed the peak of the carbonyl group apparently at  $1602\text{ cm}^{-1}$ . While the increasing TOBC contents showed peak of the carbonyl group shift toward higher wavelengths. This shift to higher wavelengths could be attributed to the carboxylic groups on TOBC surface linking adjacent alginate molecules to form the cross-linked network. This change suggested the evidence of ionic interactions and molecular compatibility between alginate and TOBC.

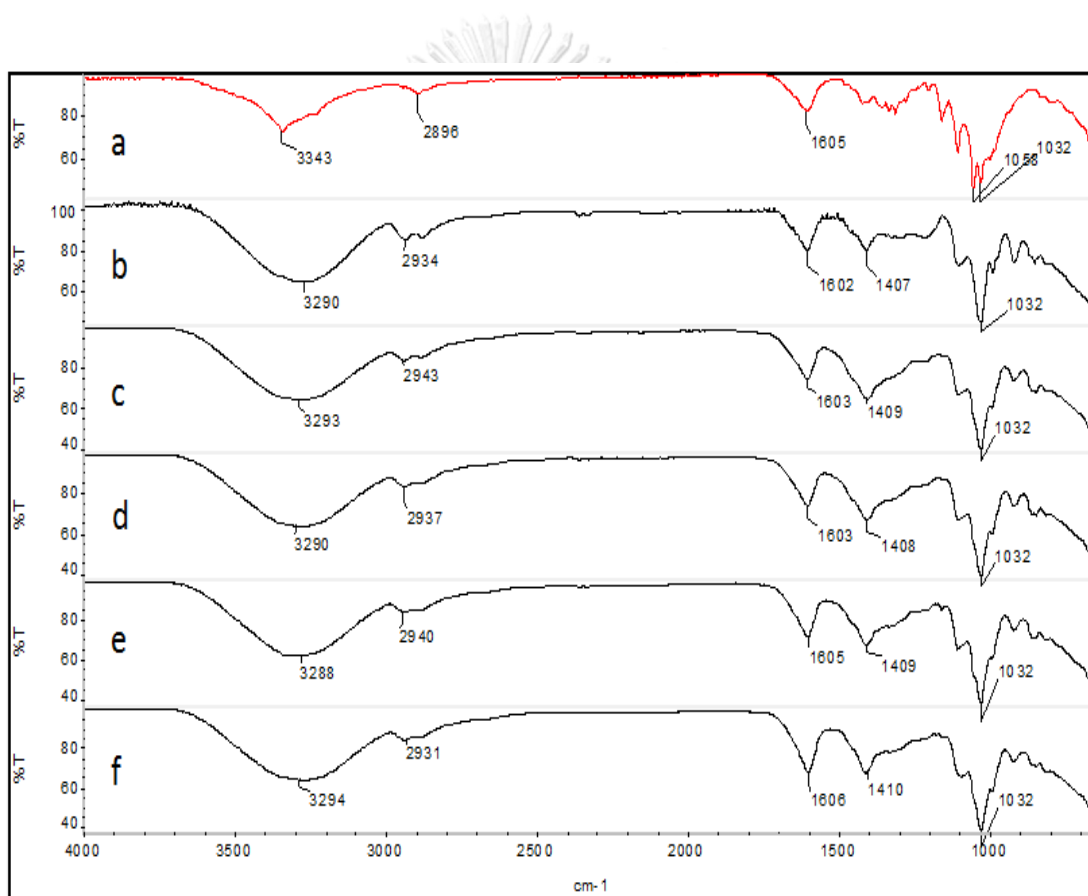


**Figure 4.11** FT-IR spectra of TOBC (a) and alginate films containing 0% (b), 0.12% (c), 0.25% (d), 0.50% (e), and 0.75 %w/v (f) of TOBC in 1%w/v alginate solution.

#### 4.3.4 Thermal gravimetric analysis (TGA)

The TGA of TOBC and films gave the thermogravimetric (TG) (Appendix D) and thermogravimetric derivative (DTG) curves (Fig. 4.12). The DTG analysis was use for



evaluating the thermal stability of samples. The curve of alginate film showed first weight loss in a temperature range from 36 to 140 °C corresponded to the evaporation of absorbed water. The second temperature drop stage at 140 °C to 280 °C was due to the thermal destruction of the glycosidic bonds of alginate. TOBC had weight loss in the temperature range of 200 °C to 340 °C ascribed to the destruction of the glycosidic bonds. The alginate films with 0.12-0.50% TOBC showed major peaks of alginate at 215 °C and of TOBC at 302.3 °C. The degradation temperature ( $T_{deg}$ ) of TOBC in film matrix was different from the neat TOBC due to the interaction between TOBC and alginate. Moreover, the enhancement of this interaction was observed in 0.75% TOBC-alginate film which  $T_{deg}$  of alginate and TOBC shifted to be 209 and 329.6 °C, respectively. Therefore, the thermal properties of TOBC-alginate films were not significantly different from alginate film.

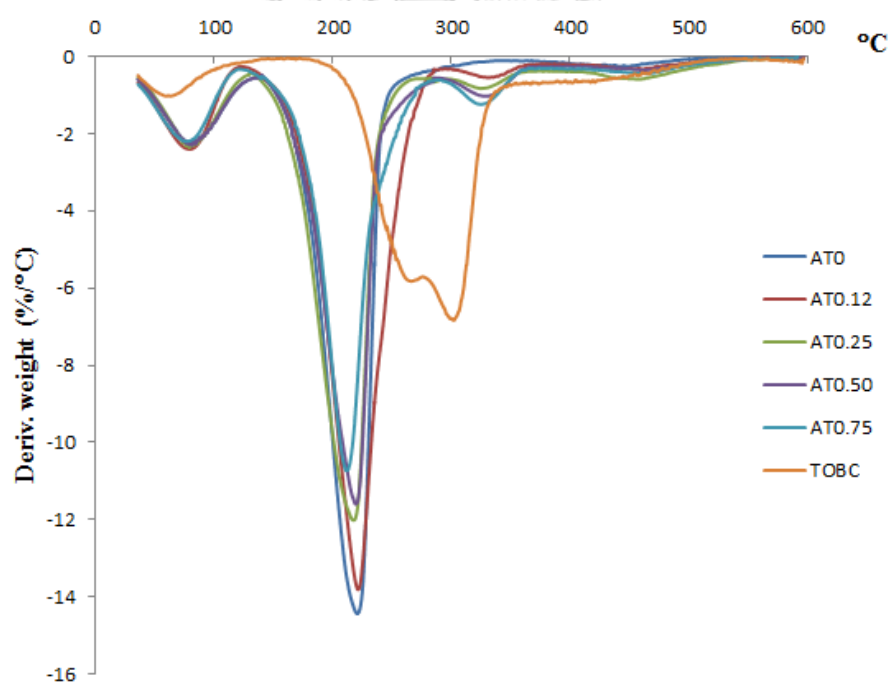


**Figure 4.12** DTG analysis of TOBC-alginate films.

#### 4.3.5 Water vapor transmission rate (WVTR)

The mechanism of water vapor transmission (WVTR) is a diffusion process in which water vapor condenses and dissolves on the film surface and then liquid

water diffuses through the film. Typically, alginate film has poor moisture barriers since they are hydrophilic films. In this study, the result in Table 4.3 showed that various TOBC in alginate films was not affected the WVTR of alginate film.

**Table 4.3** The water vapor transmission (WVTR) of TOBC-alginate films.

Time (Days)	Water vapor transmission rate (g/cm <sup>2</sup> )									
	AT0		AT0.12		AT0.25		AT0.50		AT0.75	
	Mean	SD	Mean	SD	Mean	SD	Mean	SD	Mean	SD
1	11.17	0.58	12.64	0.34	12.97	0.84	11.24	1.97	12.20	1.10
2	21.42	0.56	24.25	0.94	23.88	1.19	22.18	2.44	22.50	0.81
3	33.42	1.23	36.74	0.10	36.14	1.27	34.23	3.29	35.07	0.55
4	43.79	1.29	48.12	0.36	47.10	1.05	44.55	4.00	45.7	0.17
5	51.71	1.15	57.07	0.92	55.44	0.27	53.56	4.50	54.20	0.41
6	63.22	1.90	68.52	0.08	67.06	0.45	64.68	5.73	66.30	1.15
7	74.67	2.36	80.25	0.03	78.63	0.27	76.34	6.91	78.97	1.19

#### 4.3.6 Oxygen transmission rate (OTR)

Oxygen transmission rate (OTR) is the gas amount measurement that passes through composite film. Oxygen causes the food oxidation led to odor, color, flavor, and nutrient deterioration. Composite films with proper oxygen barrier can help improving food quality and extending food shelf-life. The result of this study revealed that at least 0.50% TOBC can enhance the OTR of alginate films. The AT0.50 and AT0.75 films had 3- and 6-fold OTR better than control film, respectively. This can explain by SEM and XRD analysis that these films had tightly packed matrix and high crystallinity which can prevent gas permeability through the films.

**Table 4.4** The Oxygen transmission rate (OTR) of TOBC-alginate films.

Alginate films contain TOBC (%)	Oxygen permeability rate (cm <sup>3</sup> /m <sup>2</sup> .d.bar)*
0	4.70
0.12	3.16
0.25	4.69
0.50	1.56
0.75	0.81

\* %RPD less than 10%



## CHAPTER V

### CONCLUSION

This study reported the examination of preparing oil loaded alginate (OA) capsules which was expected to be a new prototype of alternative capsules. The capsule shell was the mixture of alginate and Tempo-oxidized bacterial cellulose (TOBC) whereas rice bran oil is the capsule core. Using a coaxial-glass tube, alginate capsules formed by cross-linking with  $\text{Ca}^{2+}$  and TOBC was a reinforcement additive. TOBC with the degree of substitution of 0.15 were obtained by TEMPO-mediated oxidation to introduce carboxylate groups on BC surfaces. The XRD analysis revealed the decrease of crystallinity of TOBC comparing to that of BC. This might be due to the carboxyl groups on the TOBC caused the repulsive interaction between adjacent fibers. However, TOBC had better aqueous dispersion than unmodified BC.

The factors that influenced on the shape and production efficiency of capsules was first examined. The 5 and 10 cm gap (between tube tip and the  $\text{Ca}^{2+}$  ions bath) gave the higher %capsule formation efficiency (CFE) than 20 cm gap. At the same gap, the increasing amount of TOBC led to increase the viscosity of shell solution, and resulting in the decreasing of %CFE. However, the gap and viscosity of shell viscosity had no effect on the size and shell thickness of capsules. Most capsules had the size and shell thickness in a same range of 4.2-4.6 mm and 0.3-0.4, respectively. Increasing of TOBC content enhanced the turbidity of shell but gave smoother surface. At the amount of 0.50-0.75 %w/v of TOBC, capsules exhibited the higher compression strength whereas, at lower than that, the TOBC amount was not increase the compression strength. Fabricated OA capsules had the compression strength in a range of 0.04-0.12 MPa which can be classified as soft capsules (0.02-0.41 MPa).

The TOBC-alginate film was fabricated to easier characterization the shell property. The addition of TOBC affected the turbidity and surface as the capsule experiment. More TOBC content can decrease the shrinkage of films. The good mechanical property of films was found at the 0.5-0.75% of TOBC content which

correlated to the good arrangement of film matrix examined by SEM and XRD techniques. The carboxyl group of TOBC can participate crosslinking with  $\text{Ca}^{2+}$  and act as the structural construction of the alginate. The thermal and water vapor transmission rate (WVTR) properties of TOBC-alginate films were not significantly different from alginate film. At least of 0.50% of TOBC can improve the oxygen transmission rate (OTR) values of TOBC-alginate films.

In conclusion, this study was successful to fabricate the rice bran oil loaded alginate capsules using a coaxial glass-tube. The TOBC was well dispersion in alginate solution and be used as the reinforcement agent to improve the mechanical property and OTR of alginate shell.



## REFERENCES

- [1] Qiu, Y., Chen, Y., Zhang, G.G.Z., Yu, L., and Mantri, R.V. Chapter 27 - Capsules Dosage Form: Formulation and Manufacturing Considerations. Developing Solid Oral Dosage Forms (Second Edition) (2017): 723-747.
- [2] Oladzadabbasabadi, N., Ebadi, S., Mohammadi Nafchi, A., Karim, A.A., and Kiahosseini, S. Functional properties of dually modified sago starch/ $\kappa$ -carrageenan films: An alternative to gelatin in pharmaceutical capsules. Carbohydrate Polymers 160 (2017): 43-51.
- [3] Zhang, Y., Zhao, Q., Wang, H., Jiang, X., and Cha, R. Preparation of green and gelatin-free nanocrystalline cellulose capsules. Carbohydrate Polymers 164 (2017): 358-363.
- [4] Tanabe, S., Hase, M., Yano, T., Sato, M., Fujimura, T., and Akiyama, H. A real-time quantitative PCR detection method for pork, chicken, beef, mutton, and horseflesh in foods. Biosci Biotechnol Biochem 71(12) (2007): 3131-5.
- [5] A. Morrison, N., C. Clark, R., L. Chen, Y., Talashek, T., and Sworn, G. Gelatin alternatives for the food industry : recent developments, challenges and prospects. Trends in Food Science & Technology 19(12) (2008): 644-656.
- [6] Boontheekul, T., Kong, H.J., and Mooney, D.J. Controlling alginate gel degradation utilizing partial oxidation and bimodal molecular weight distribution. Biomaterials 26(15) (2005): 2455-65.
- [7] Fertah, M. Chapter 2 - Isolation and Characterization of Alginate from Seaweed. Seaweed Polysaccharides (2017): 11-26.
- [8] Wu, J., et al. Fabrication and characterization of monodisperse PLGA–alginate core–shell microspheres with monodisperse size and homogeneous shells for controlled drug release. Acta Biomaterialia 9(7) (2013): 7410-7419.
- [9] Phawaphuthanon, N., Behnam, S., Koo, S., Pan, C., and Chung, D. Characterization of core–shell calcium-alginate macrocapsules fabricated by electro-coextrusion. International Journal of Biological Macromolecules 65 (2014): 267-274.

- [10] Del Gaudio, P., et al. Novel co-axial prilling technique for the development of core-shell particles as delayed drug delivery systems. European Journal of Pharmaceutics and Biopharmaceutics 87(3) (2014): 541-547.
- [11] Moghaddam, M., Mortazavi, S., and Khayamian, T. Preparation of calcium alginate microcapsules containing n-nonadecane by a melt coaxial electrospray method. Journal of Electrostatics 73 (2015): 56-64.
- [12] Smidsrod, O. and Skjak-Braek, G. Alginate as immobilization matrix for cells. Trends in biotechnology 8(3) (1990): 71-8.
- [13] Rowley, J.A., Madlambayan, G., and Mooney, D.J. Alginate hydrogels as synthetic extracellular matrix materials. Biomaterials 20(1) (1999): 45-53.
- [14] Daemi, H. and Barikani, M. Synthesis and characterization of calcium alginate nanoparticles, sodium homopolymannuronate salt and its calcium nanoparticles. Scientia Iranica 19(6) (2012): 2023-2028.
- [15] Grant, G.T., Morris, E.R., Rees, D.A., Smith, P.J.C., and Thom, D. Biological interactions between polysaccharides and divalent cations: The egg-box model. FEBS Letters 32(1) (1973): 195-198.
- [16] Kühbeck, D., Mayr, J., Häring, M., Hofmann, M., Quignard, F., and Díaz Díaz, D. Evaluation of the nitroaldol reaction in the presence of metal ion-crosslinked alginates. New Journal of Chemistry 39(3) (2015): 2306-2315.
- [17] Lee, K.Y. and Mooney, D.J. Alginate: properties and biomedical applications. Progress in polymer science 37(1) (2012): 106-126.
- [18] Shilpa, A., Agrawal, S.S., and Ray, A.R. Controlled Delivery of Drugs from Alginate Matrix. Journal of Macromolecular Science, Part C 43(2) (2003): 187-221.
- [19] Chan, L.W., Lee, H.Y., and Heng, P.W.S. Mechanisms of external and internal gelation and their impact on the functions of alginate as a coat and delivery system. Carbohydrate Polymers 63(2) (2006): 176-187.
- [20] Benavides, S., Cortés, P., Parada, J., and Franco, W. Development of alginate microspheres containing thyme essential oil using ionic gelation. Food Chemistry 204 (2016): 77-83.
- [21] Morales, E., Rubilar, M., Burgos-D., Acevedo, F., Penning, M., and Shene, C. Alginate/Shellac beads developed by external gelation as a highly efficient

- model system for oil encapsulation with intestinal delivery. Food Hydrocolloids 70 (2017): 321-328.
- [22] Leong, J., et al. Advances in fabricating spherical alginate hydrogels with controlled particle designs by ionotropic gelation as encapsulation systems. Particuology 24 (2016): 44-60.
- [23] Liu, X.D., et al. Characterization of structure and diffusion behaviour of Ca-alginate beads prepared with external or internal calcium sources. Journal of microencapsulation 19(6) (2002): 775-82.
- [24] Chan, L.W., Lee, H.Y., and Heng, P.W.S. Production of alginate microspheres by internal gelation using an emulsification method. International Journal of Pharmaceutics 242(1) (2002): 259-262.
- [25] Quong, D., Neufeld, R.J., Skjak-Braek, G., and Poncelet, D. External versus internal source of calcium during the gelation of alginate beads for DNA encapsulation. Biotechnology and bioengineering 57(4) (1998): 438-46.
- [26] Choi, B.Y., Park, H.J., Hwang, S.J., and Park, J.B. Preparation of alginate beads for floating drug delivery system: effects of CO<sub>2</sub> gas-forming agents. International Journal of Pharmaceutics 239(1) (2002): 81-91.
- [27] Abang, S., Chan, E.S., and Poncelet, D. Effects of process variables on the encapsulation of oil in ca-alginate capsules using an inverse gelation technique. Journal of microencapsulation 29(5) (2012): 417-28.
- [28] Lopez, M.D., Maudhuit, A., Pascual-Villalobos, M.J., and Poncelet, D. Development of Formulations to Improve the Controlled-Release of Linalool to Be Applied As an Insecticide. Journal of Agricultural and Food Chemistry 60(5) (2012): 1187-1192.
- [29] Martins, E., Poncelet, D., and Renard, D. A novel method of oil encapsulation in core-shell alginate microcapsules by dispersion-inverse gelation technique. Journal Reactive and Functional Polymers 114 (2017): 49-57.
- [30] Martins, E., Renard, D., Davy, J., Marquis, M., and Poncelet, D. Oil core microcapsules by inverse gelation technique. Journal of microencapsulation 32(1) (2015): 86-95.
- [31] Duconseille, A., Astruc, T., Quintana, N., Meersman, F., and Sante-Lhoutellier, V.



- Gelatin structure and composition linked to hard capsule dissolution: A review. Food Hydrocolloids 43 (2015): 360-376.
- [32] Chong, R.H., Jones, B.E., Diez, F., Birchall, J.C., and Coulman, S.A. Evaluating the sensitivity, reproducibility and flexibility of a method to test hard shell capsules intended for use in dry powder inhalers. International journal of pharmaceutics 500(1-2) (2016): 316-25.
- [33] Oishi, S., et al. New scale-down methodology from commercial to lab scale to optimize plant-derived soft gel capsule formulations on a commercial scale. International journal of pharmaceutics 535(1-2) (2018): 371-378.
- [34] Dagadiye, R.B., Kajale, A.D., Mahajan, V.K., and Joshi, M.H. gelatin and non gelatin capsule shell. International Journal of Advances in Pharmaceutical Research 3(10) (2012): 1178 – 1187.
- [35] Shimokawa, Y., Hayakawa, E., Takahashi, K., Okai, K., Hattori, Y., and Otsuka, M. Pharmaceutical formulation analysis of gelatin-based soft capsule film sheets using near-infrared spectroscopy. Journal of Drug Delivery Science and Technology 48 (2018): 174-182.
- [36] Eqbal, M.D. and Gundabala, V. Controlled fabrication of multi-core alginate microcapsules. Journal of Colloid and Interface Science 507 (2017): 27-34.
- [37] Pommet, M., et al. Surface Modification of Natural Fibers Using Bacteria: Depositing Bacterial Cellulose onto Natural Fibers To Create Hierarchical Fiber Reinforced Nanocomposites. Biomacromolecules 9(6) (2008): 1643-1651.
- [38] Tayeb, A., Amini, E., Ghasemi, S., and Tajvidi, M. Cellulose Nanomaterials—Binding Properties and Applications: A Review. Molecules 23(10) (2018): 2684.
- [39] Vijayabaskaran, T. and Vitta, S. Ni-bacterial cellulose nanocomposite; A magnetically active inorganic-organic hybrid gel. RSC Advances 3(31) (2013): 12765-12773.
- [40] Tahara, N., Tabuchi, M., Watanabe, K., Yano, H., Morinaga, Y., and Yoshinaga, F. Degree of Polymerization of Cellulose from *Acetobacter xylinum* BPR2001 Decreased by Cellulase Produced by the Strain. Bioscience, biotechnology, and biochemistry 61(11) (1997): 1862-5.
- [41] Svensson, A., et al. Bacterial cellulose as a potential scaffold for tissue

- engineering of cartilage. Biomaterials 26(4) (2005): 419-431.
- [42] Florea, M., Reeve, B., Abbott, J., Freemont, P.S., and Ellis, T. Genome sequence and plasmid transformation of the model high-yield bacterial cellulose producer *Gluconacetobacter*. Scientific reports 6 (2016): 23635.
- [43] Kirdponpattara, S., Khamkeaw, A., Sanchavanakit, N., Pavasant, P., and Phisalaphong, M. Structural modification and characterization of bacterial cellulose-alginate composite scaffolds for tissue engineering. Carbohydrate Polymers 132 (2015): 146-155.
- [44] Wang, X., et al. Development and characterization of bacterial cellulose reinforced biocomposite films based on protein from buckwheat distiller's dried grains. International Journal of Biological Macromolecules 96 (2017): 353-360.
- [45] Jia, Y., Wang, X., Huo, M., Zhai, X., Li, F., and Zhong, C. Preparation and characterization of a novel bacterial cellulose/chitosan bio-hydrogel. Nanomaterials and Nanotechnology 7 (2017): 1847-9804.
- [46] Park, M., Lee, D., and Hyun, J. Nanocellulose-alginate hydrogel for cell encapsulation. Carbohydrate Polymers 116 (2015): 223-228.
- [47] Elayaraja, S., Zagorsek, K., Li, F., and Xiang, J. In situ synthesis of silver nanoparticles into TEMPO-mediated oxidized bacterial cellulose and their antibiotoxic activity against shrimp pathogens. Carbohydrate Polymers 166 (2017): 329-337.
- [48] Jia, Y., Zhai, X., Fu, W., Liu, Y., Li, F., and Zhong, C. Surfactant-free emulsions stabilized by tempo-oxidized bacterial cellulose. Carbohydrate Polymers 151 (2016): 907-915.
- [49] Isogai, A., Saito, T., and Fukuzumi, H. TEMPO-oxidized cellulose nanofibers. Nanoscale 3(1) (2011): 71-85.
- [50] Rohaizu, R. and Wanrosli, W.D. Sono-assisted TEMPO oxidation of oil palm lignocellulosic biomass for isolation of nanocrystalline cellulose. Ultrasonics Sonochemistry 34 (2017): 631-639.
- [51] Lin, N., Bruzzese, C., and Dufresne, A. TEMPO-Oxidized Nanocellulose Participating as Crosslinking Aid for Alginate-Based Sponges. ACS Applied Materials & Interfaces 4(9) (2012): 4948-4959.

- [52] Shen, X., Huang, P., Chen, J., Wu, Y., Liu, Q., and Sun, R. Comparison of Acid-hydrolyzed and TEMPO-oxidized Nanocellulose for Reinforcing Alginate Fibers. BioResources 12 (2017): 8180-8198.
- [53] Abouzeid, R.E., Khiari, R., Beneventi, D., and Dufresne, A. Biomimetic Mineralization of Three-Dimensional Printed Alginate/TEMPO-Oxidized Cellulose Nanofibril Scaffolds for Bone Tissue Engineering. Biomacromolecules 19(11) (2018): 4442-4452.
- [54] Luo, H., et al. Characterization of TEMPO-oxidized bacterial cellulose scaffolds for tissue engineering applications. Materials Chemistry and Physics 143(1) (2013): 373-379.
- [55] Woggum, T., Sirivongpaisal, P., and Wittaya, T. Properties and characteristics of dual-modified rice starch based biodegradable films. International Journal of Biological Macromolecules 67 (2014): 490-502.
- [56] Spatafora, A., Sáenz, P., Mújica, H., and Valdez, A. External factors and nanoparticles effect on water vapor permeability of pectin-based films. Journal of Food Engineering 245 (2019): 73-79.
- [57] Naseri, N., Deepa, B., Mathew, A.P., Oksman, K., and Girandon, L. Nanocellulose-Based Interpenetrating Polymer Network (IPN) Hydrogels for Cartilage Applications. Biomacromolecules 17(11) (2016): 3714-3723.
- [58] Chan, E.S., Lee, B., Ravindra, P., and Poncelet, D. Prediction models for shape and size of ca-alginate macrobeads produced through extrusion-dripping method. Journal of Colloid and Interface Science 338(1) (2009): 63-72.



APPENDIX

จุฬาลงกรณ์มหาวิทยาลัย  
**CHULALONGKORN UNIVERSITY**

APPENDIX A

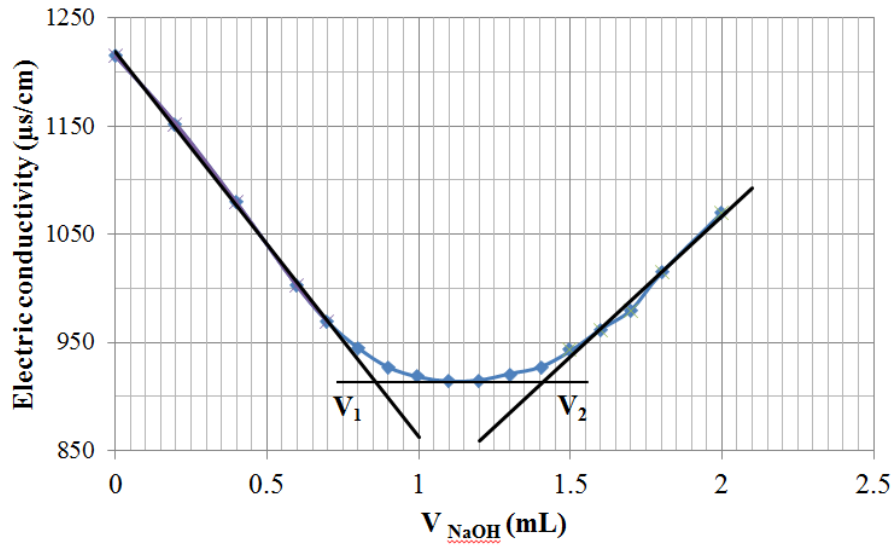


Figure A1 Titration curve of TOBC.

## APPENDIX B

**Table B1** The light transmittance percentages of all films.

films	% Light transmittance		
AT0	45.21	46.08	46.95
AT0.12	22.53	23.31	24.09
AT0.25	3.83	4.21	4.59
AT0.50	1.65	2.3	2.95
AT0.75	1.50	1.77	2.04

APPENDIX C

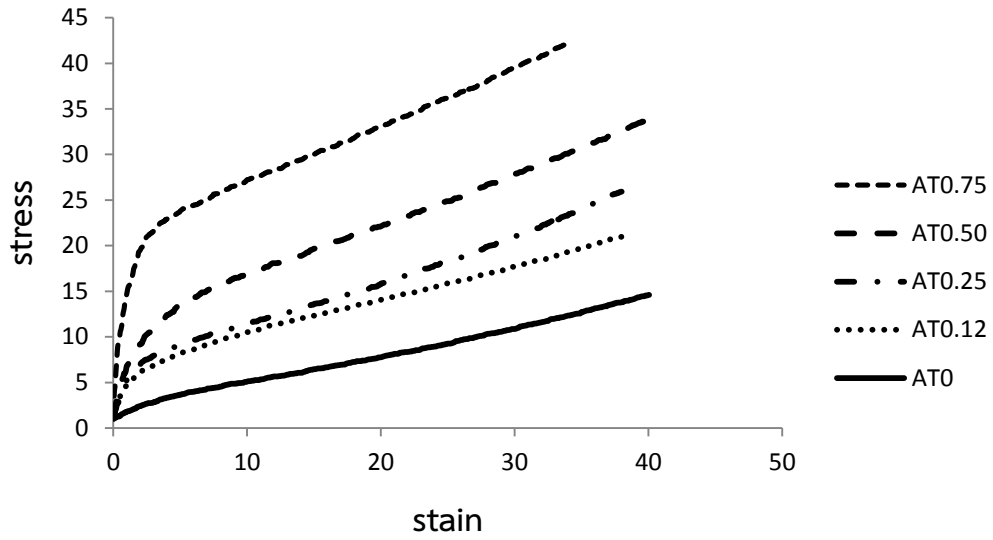


Figure C1 The stress/strain curve of all films.



## APPENDIX D

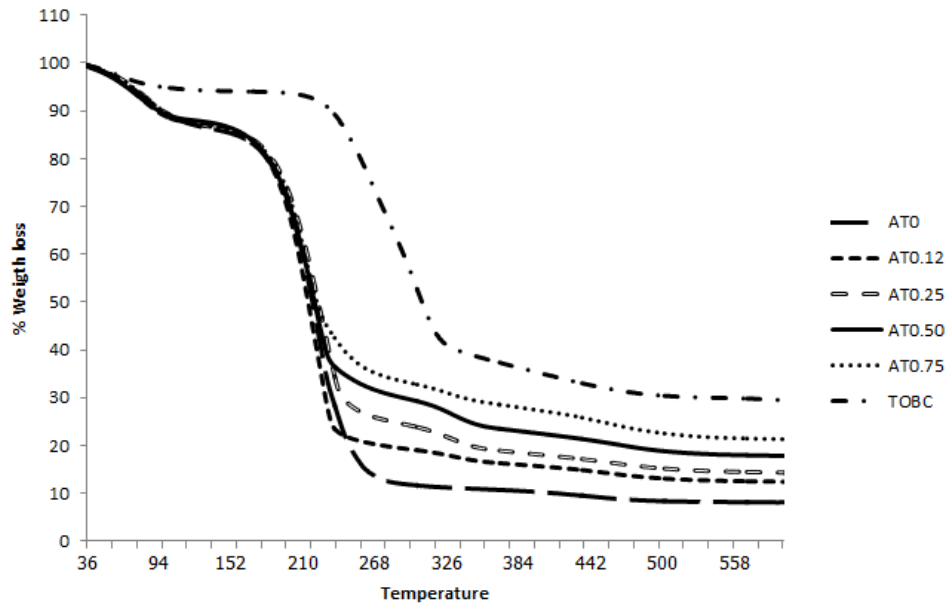


Figure D1 The thermogravimetric (TG) of TOBC and all films.







จุฬาลงกรณ์มหาวิทยาลัย  
**CHULALONGKORN UNIVERSITY**

## VITA

**NAME** Panida Watchanung

**DATE OF BIRTH** 26 August 1992

**PLACE OF BIRTH** Suratthani

**INSTITUTIONS ATTENDED** Bachelor's Degree from Department of Chemistry, Faculty of Science, Thammasat University, 2011-2015. Master's Degree from Program in Petrochemistry and polymer science, Faculty of Science, Chulalongkorn University.

**HOME ADDRESS** 44, Moo. 7, Lamed, Chaiya, Suratthani, 84110

**PUBLICATION** Conference attendance : Poster presentation "TEMPO-oxidized bacterial cellulose for reinforcing alginate-based films " at the Congress on Science and Technology of Thailand (STT 2018), bangkok international trade & exhibition center (BITEC), Bangkok , Thailand, 29-31 October 2018.